LA-UR-16-26714
Approved for public release; distribution is unlimited.

Title: Progress, Performance, and Prospects of Ultra-High Resolution Microcalorimeter Spectrometers

Author(s): Hoover, Andrew Scott
Bennett, D. A.
Croce, Mark Philip
Rabin, Michael W.
Ullom, J. N.

Intended for: Report

Issued: 2017-01-23 (rev.1)

Progress, Performance, and Prospects of Ultra-High Resolution Microcalorimeter Spectrometers
LA-UR-16-26714

A.S. Hoover[1], D.A. Bennett[2] , M.P. Croce[1], M.W. Rabin[1], J.N. Ullom[2,3]

[1]Los Alamos National Laboratory, Los Alamos, NM
[2]National Institute of Standards and Technology, Boulder, CO
[3]University of Colorado, Boulder, CO

August 29, 2016

1. Summary

In 2005 the LANL/NIST team used a single high-resolution microcalorimeter detector to measure the gamma-ray spectrum of a plutonium sample. After more than a decade of research and development on this topic, both the technology and our general understanding of its capabilities have advanced greatly, such that a progress review is now timely.

We examine the scenario of a large-scale reprocessing plant and conclude that current non-destructive analysis (NDA) methods are inadequate to safeguard such a facility to the desired levels, leading to undesirable dependence on mass-spectrometry (MS) destructive analysis (DA). The development of microcalorimeter detectors is intended to close the performance gap between NDA and DA methods to address the needs of nuclear facilities.

The microcalorimeter technology has advanced rapidly in the past decade, moving from a single pixel proof-of-concept experiment, to an array of hundreds of pixels collecting spectra with tens of millions of counts. Order-of-magnitude improvement in energy resolution over conventional high-purity germanium (HPGe) detectors is now established and repeatable. Larger and faster sensor arrays with thousands of active pixels providing increased detection efficiency and reduced count times are practically achievable with technologies currently in hand or nearly so. Current development of microwave multiplexing is a critical component of the path to larger arrays.

Our understanding of the inverse spectral problem (extracting peak areas and isotope ratios from measured spectral data) has also advanced significantly. Much more is now known about the critical metric of total measurement uncertainty, what improvement is gained by the increased resolution of microcalorimeters, and what factors continue to ultimately limit the performance. While the resolution performance of microcalorimeters is impressive, direct translation to equivalent improvement in total measurement uncertainty is more complicated. We find that measurement uncertainty limits are not only dependent on sensor performance, instead containing significant and sometimes dominant contributions from other factors required for spectral analysis such as the use of fitting models, and required external knowledge like constants of nature (gamma-ray branching fractions, energies, etc.). We argue that improved nuclear data

(particularly of gamma-ray branching fractions) is highly desirable, along with exploration of possible ways to reformulate the spectral analysis problem itself. For improving nuclear data, the microcalorimeter technology itself may be best suited to the task, as the high energy-resolution could allow for better measurement of x-ray line widths and gamma-ray energies. Microcalorimeter data could also improve the performance of conventional HPGe detectors, by providing detailed measurements to constrain parameters (e.g. - relative peak heights) of lower resolution HPGe analysis, or better x-ray line width and gamma-ray energy values.

In the applications area, we identify a number of points within a fuel reprocessing stream where microcalorimeter technology appears well-suited, utilizing both gamma-ray and x-ray measurements. These include head-end measurement of Pu content in the fuel, and isotopic and total Pu measurement of aqueous solutions, oxide powders, MOX pellet output, and waste materials. An attractive location for our first measurements at a real, operational nuclear facility is the H-canyon reprocessing plant and associated F/H-canyon analytical laboratory at the Savannah River Site (SRS). Such measurements are likely in the next few years under a recently funded NEUP proposal.

Microcalorimeter gamma-ray spectroscopy is still in its infancy compared to HPGe spectroscopy, which has had 40 years to mature. Achieving our goal of determining elemental and isotopic fractions with relative uncertainty below 1% using microcalorimeters will create a new safeguards paradigm since slow, preparation-intensive DA testing can be replaced by rapid NDA. While prior progress has been rapid and impressive, significant work remains. The recommended path forward includes continued development of improved arrays, work to reduce total measurement uncertainty, and measurements at a real operational nuclear facility. Sensor and readout hardware continues to advance at a rapid pace, and thousand-pixel arrays are practically assured in the future. On the topic of reducing total measurement uncertainty, the challenges are of a different nature and the path forward is less well-prescribed. The accumulation of more high-statistics data from more samples, and a fresh, critical look at conventional analysis methods are called for. For demonstration measurements, the F/H-canyon analytical laboratory at SRS is the logical location.

2. Motivation

Nuclear safeguards are comprised of all activities used to assess the degree to which a nuclear activity (process), nuclear facility, interrelated set of facilities and activities, or an entire state is in compliance with legitimate use. Nuclear materials and activities accounting detect potential diversion or theft of potentially significant quantities of nuclear materials. The modern safeguards approach attempts to assess the entire nuclear fuel cycle. Many of the technologies in use for safeguards measurements today are the results of research and development programs from the 1980s [Scheinman, 2009]. New requirements are emerging in an evolving landscape that includes large-scale commercial reprocessing and pyroprocessing. Development of sustainable nuclear fuel cycles that include reprocessing of large

quantities of irradiated fuel will require innovative solutions to meet modern safeguards challenges.

The work described here is principally directed at Pu measurement in the context of a fuel reprocessing plant, though there is nothing precluding application of the technology to other aspects of the nuclear enterprise (e.g. – U measurements). A range of measurement techniques and instruments are available depending on the type and amount of material available for examination, and the nature of the measurement environment. Passive NDA by gamma-ray spectroscopy is one such analytical method. It was recognized that superconducting microcalorimeter detectors, providing exceptional energy resolution for x-ray and gamma-ray spectroscopy (on the order of 50 eV FWHM at 100 keV), could be applied to nuclear safeguards and could potentially significantly improve the performance of certain categories of measurements [Rabin, 2009].

For the isotopes principally of interest in the context of irradiated fuel reprocessing ($^{238\text{-}242}$Pu), the relatively small branching fractions for gamma-ray emission (typically less than 10^{-4}) imply that gamma-ray spectroscopy is primarily relevant for the analysis of bulk samples having total mass on the order of 0.1 gram or more, where the total emission rate is practical for radiometric methods. Generally, NDA methods are preferred to avoid time-intensive radiochemistry separations and waste products associated with DA. In the realm of NDA of bulk samples by gamma-ray spectroscopy, high-purity germanium (HPGe) has been the gold-standard measurement technique for several decades. Its advantages include high resolution (~500 eV FWHM at 100 keV), high efficiency, and relatively simple operation (single-channel readout with conventional preamp hardware). For a low uncertainty measurement, the 100 keV spectral region (in actuality extending up to the 208 keV line of ^{241}Pu/^{241}Am) is used as it provides an order of magnitude higher emission rate than other gamma-ray lines in higher energy spectral regions, and it contains emissions from every Pu isotope of interest (although the ^{242}Pu signal is too weak to be quantified by conventional passive gamma-ray spectroscopy).

Isotopic analysis of bulk samples by gamma-ray spectroscopy in the 100 keV region was advanced in the 1980s with great success, driven by the good HPGe energy resolution and the development of techniques allowing the effective efficiency of the source-detector system to be determined from the measured data [Sampson, 1989]. Today, target uncertainty values for HPGe analysis are in the range 1 – 7 % (total random and systematic error, 3000 seconds, 0.5 g Pu) depending on the isotope ratio and material enrichment [Zhao, 2012]. In some cases HPGe analysis is competitive with DA methods. In particular for the ^{238}Pu/^{239}Pu ratio which presents a challenge to MS due to the isobaric interference of ^{238}U and ^{238}Pu. In other cases the target uncertainty of HPGe is up to an order of magnitude larger than MS, as is the case for the ^{240}Pu/^{239}Pu ratio (0.1 % MS versus 1.5 % HPGe NDA for low-burnup). If we allow for very long measurement times to drive down the random error component, the HPGe systematic uncertainty target values are still in the range 0.7 – 5 %. Considering that HPGe technology is decades old, we may assume that maturity has been reached, and a total measurement uncertainty in the range 0.7 - 5 % is the practical limit for Pu isotopics using conventional technology.

The fundamental problem of high-capacity facility safeguards is that any system of accounting has systematic error that is generally proportional to the total amount of material processed in a specified time. A simple calculation oriented towards a large-scale (hundreds of metric tons annual throughput) reprocessing plant illustrates that this limit is inadequate to meet performance goals using NDA methods. Consider the problem of quantifying the total Pu mass of an object. Assume the isotope ratios are determined by gamma-spectroscopy and combined with a method for determining total activity (e.g. - neutron counting or total power calorimetry), and that the isotope ratio uncertainties are dominant. For hypothetical irradiated fuel with 1 % plutonium content, a 1 % measurement uncertainty leads to total plutonium mass uncertainty exceeding the IAEA significant quantity of 8 kg (for example, 80 kg Pu uncertainty for a 800 t/yr plant throughput containing 8000 kg Pu). Similarly, the isotopics of an output product (e.g. - MOX pellets) could not be determined with less than 1 % uncertainty. In reality, safeguards measurements of a reprocessing stream are much more complicated, but the high-level calculation illustrates the need for lower uncertainty limits.

For a long time, the best NDA technique for Pu isotopics has been HPGe. If lower uncertainty values are required one must turn to DA. Microcalorimeter detectors are envisioned as an enabling technology to lower the achievable measurement uncertainty of NDA. At a very high level, our goal is to make NDA competitive with DA. As we will see, while HPGe resolution is good, the gamma-ray lines of Pu are tightly spaced, and significant overlap of spectral peaks persists. The order-of-magnitude improvement in resolution afforded by microcalorimeter detectors greatly improves the ability to discern individual spectral peaks and should logically lead to improved quantitative analysis of the sample. While this is a simple extrapolation in theory, our actual experience has exposed a number of intermediate factors that influence the realized performance. In the following sections, we will first introduce the microcalorimeter technology and the achieved performance. Then, we summarize measurements collected on Pu reference samples, spectral analysis methods, and the study of uncertainty. Then we discuss the potential for implementation of microcalorimeters within a nuclear facility. Finally, we provide a narrative history of the project highlighting key technology advances.

<u>Key points from this section:</u>

- *The current best NDA method for Pu isotopics (HPGe gamma-ray spectroscopy) provides about 1 % measurement uncertainty at best. This is inadequate for safeguarding of large, high-throughput reprocessing plants to the desired level.*

- *The application of microcalorimeter detectors is intended to provide a new NDA technology capable of reducing total measurement uncertainty below 1 %, with the ultimate goal of being competitive with DA methods.*

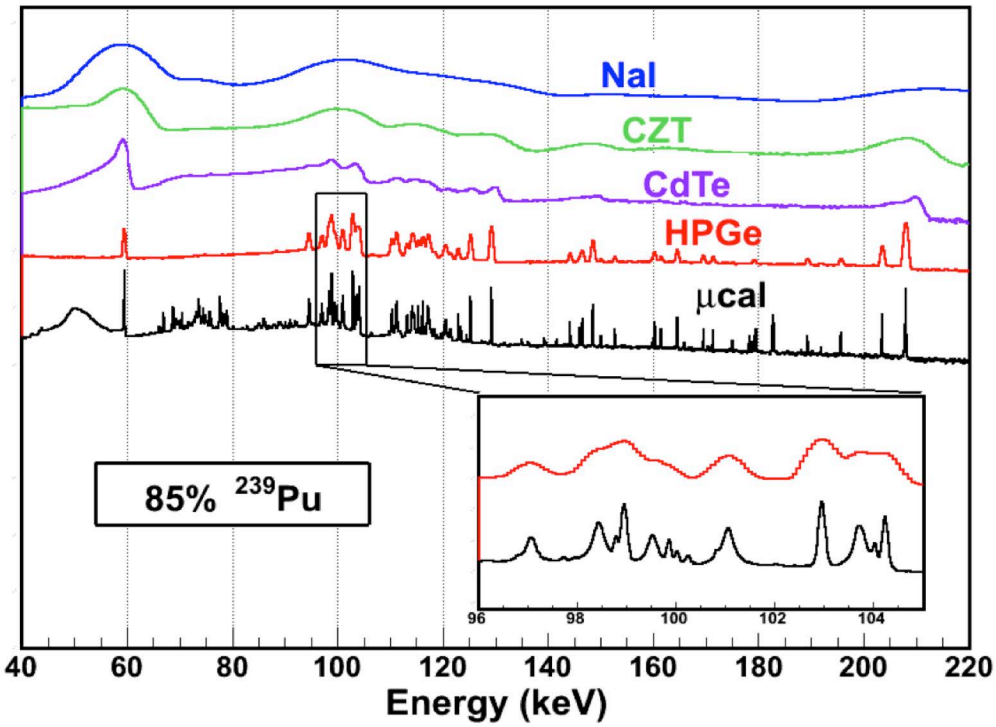

Figure 1 - A comparison of several conventional gamma-ray detection technologies with a microcalorimeter using data from a Pu sample. Microcalorimeters provide order-of-magnitude improvement in energy resolution over HPGe detectors. The inset shows the improved resolving power for the complex 100 keV region.

3. Microcalorimeter Detectors

The body of literature on superconducting microcalorimeter detectors is vast. For a good overview relevant to the present discussion the reader is referred to [Ullom, 2015]. While many variants exist, our work is focused on the transition-edge sensor (TES). TESs are thermal detectors that rely on the steep resistive transition of a superconducting material as a thermometer. The suppression of thermal noise at low temperatures enables energy or power deposited by photons and particles to be measured with great precision. In the case of x-rays and gamma-rays, the energy of single photons can be measured with resolving powers $E/\Delta E > 10^3$. This quality of spectroscopy is significantly better than can be accomplished with scintillating or even semiconducting sensors such HPGe. The energy resolution of a conventional semiconductor gamma-ray detector is fundamentally limited by the Fano statistics of electron–hole pair generation. In contrast, cryogenic microcalorimeters are fundamentally limited by thermal noise processes. A resolution comparison of several detection technologies is shown in Figure 1. Similar to the way HPGe advanced the state-of-the-art of gamma-ray spectroscopy over prior technologies, microcalorimeter detectors provide a new significant improvement over HPGe.

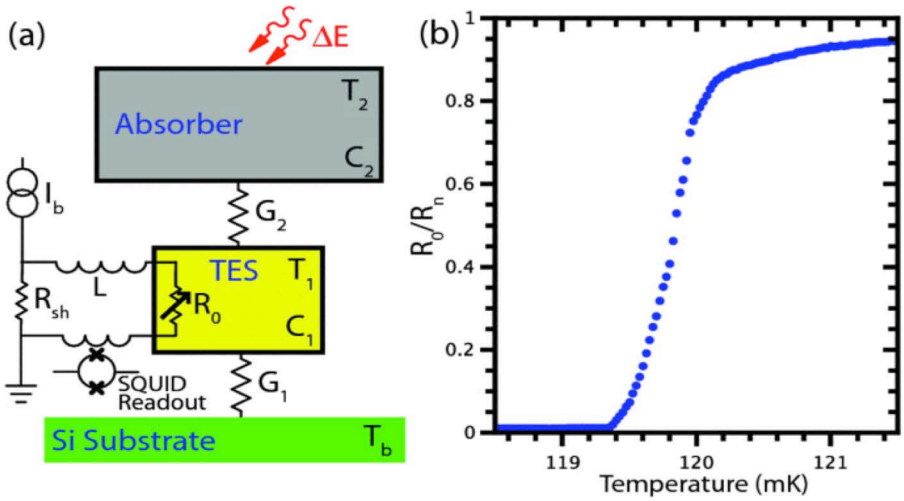

Figure 2 - (a) Conceptual schematic of microcalorimeter detector. An absorbing element is thermally coupled to a TES (G_2) and weakly coupled to a thermal bath ($G_1 < G_2$). Temperature change in the TES from an absorbed photon changes the resistance in the bias circuit, producing a magnetic field read out by a SQUID. (b) TES resistance as a fraction of the normal resistance versus temperature. The resistance changes steeply in the transition region between normal and superconducting states, resulting in a highly sensitive thermometer.

A cryogenic microcalorimeter (Figure 2) converts the energy of an incident x-ray or gamma-ray to heat. The TES itself is a thin Mo/Cu film that exhibits a steep resistive dependence on temperature in the transition region between normal and superconducting states. The properties of the transition depend on many factors. Our TESs are designed to have a transition temperature of about 100 mK with a width of about 1 mK. The TES itself has minimal stopping power for hard x-rays and gamma-rays. A bulk absorbing element is attached to the TES to stop the incident radiation. The use of tin as an absorbing element is common due to prior experience, favorable pulse decay time constants, and the fact that it is a superconductor, which leads to lower heat capacity compared to a normal material around the critical transition temperature. The most recent detectors utilize a 1.5 mm x 1.5 mm square by 0.38 mm thick tin absorber. Thermally conductive cryogenic epoxy can be used to attach the absorber. However, it was found that this produces heat trapping and long pulse decay times. The use of a metallic connecting joint was found to greatly improve thermalization times [Horansky, 2007].

The two-body absorber/TES element is placed in a voltage-biased circuit. Voltage bias is typically achieved by placing the TES in parallel with a shunt resistor that is much smaller than the resistance of the TES at its operating point. Additionally, the TES is weakly connected to a thermal bath that is slightly below the TES temperature at its operational bias point, allowing the sensor to return to thermal equilibrium after an event. TESs are almost always measured using superconducting quantum interference devices (SQUIDs) as sensitive ammeters. SQUIDs are compatible with a number of different readout implementations, are suitable for multiplexing, and have low noise, low impedance, and low power.

To summarize the basic operating principle, incident photons are stopped by the tin absorber and the energy is thermalized. The TES temperature rises, resulting

in an increased resistance and change in current flowing through the bias circuit. The change in current through the total inductance of the circuit produces a change in the induced magnetic field that is detected by the SQUID. The signal is amplified by subsequent SQUID arrays. Each absorbed photon produces a thermal pulse in the sensor that is proportional to the energy deposited. With the collection of many events the energy spectrum is measured.

Pulse decay time constants for our TES sensors are on the order of milliseconds. This translates to a maximum pulse rate of a few counts per second (cps) for a single TES before pulse pileup becomes problematic. HPGe detectors are capable of operating at tens of kcps before spectral degradation becomes apparent. Additionally, the stopping efficiency of a single microcalorimeter is orders of magnitude less than a typical planar HPGe crystal, which may have dimensions measured in centimeters. The energy resolution of the sensor scales with the heat capacity, which precludes sizing up to arbitrarily large absorber dimensions. The need for higher detection efficiency leads to the assembly of individual microcalorimeters into large arrays. From a single-pixel experiment in 2005, the technology was rapidly scaled up to a 256-pixel array in 2009 (read "pixel" as a single TES/absorber detector).

The development of microcalorimeter arrays necessitates the incorporation of multiplexed readout schemes. Electronic division of the sensors into M columns and N rows reduces the total number of signal lines to MxN from M+N if all sensors were read out individually. Many approaches are possible for array multiplexing, including time-domain, frequency-domain, code-domain, and microwave-resonator based. For comparison of these the reader is again referred to [Ullom, 2015]. Our work has incorporated time-domain multiplexing (TDM), largely because it had the highest level of technical maturity when the work began. Details of the TDM circuitry and operation are beyond the scope of this review, and the reader is referred to [Bennett, 2012] and [Ullom, 2015]. At a summary level, the 256-pixel array is divided into 8 columns and 32 rows. The columns are read out simultaneously, while each row address is switched on and off sequentially to continuously cycle through the 32 pixels in each column. The speed of this cycling is important because it is necessary to keep the total signal voltage difference between successive time samples of a row address within allowable limits. A per-pixel sample period of 20.48 microseconds was achieved in the most recent hardware configuration, and this was very near the level required to successfully multiplex all the sensors reliably. Subsequent work on other instruments has already improved on this by a factor of 4. Robust TDM performance of a 256-pixel or even larger array is technically well in-hand.

Recent work has focused on the development of microwave SQUID multiplexing (see the SLEDGEHAMMER instrument) [Bennett, 2014]. Microwave multiplexing has the potential to provide significantly more readout bandwidth than conventional techniques by allowing many sensors to be coupled to a common feed line with simultaneous readout on a single wire. This bandwidth can be used to multiplex larger numbers of sensors or alternatively allow each sensor to have a significantly higher bandwidth. [Noroozian, 2013] performed a two-pixel demonstration of microwave SQUID multiplexing where two gamma-ray TESs were

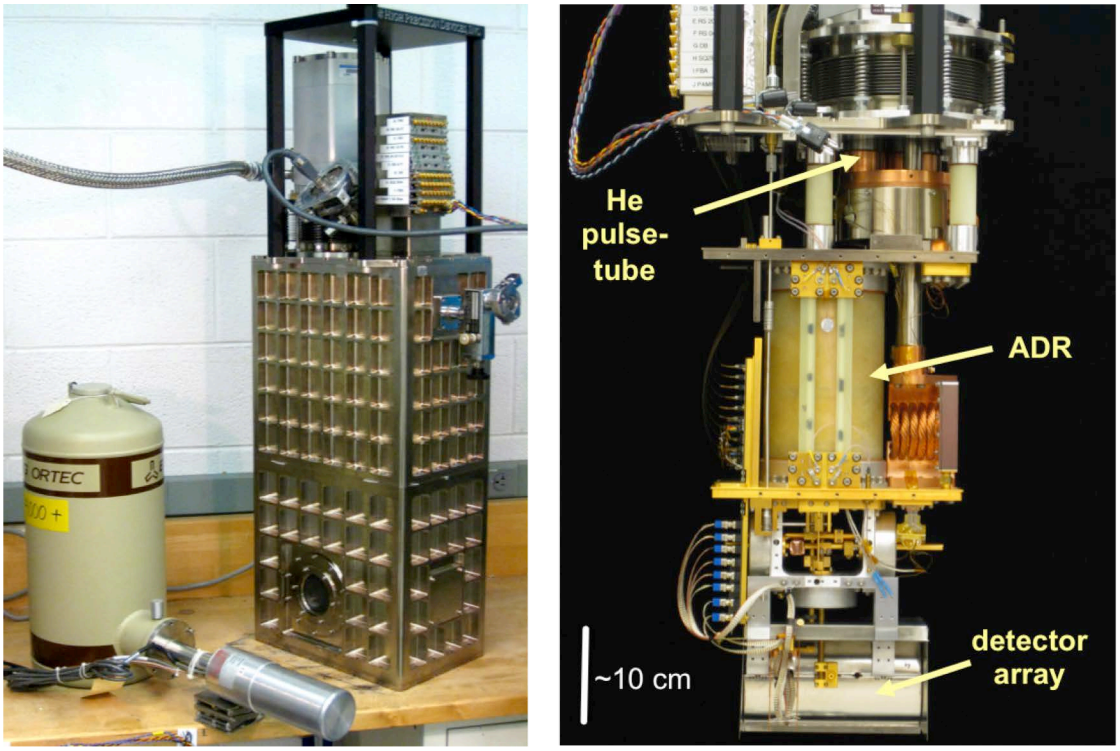

Figure 3 – At left is an external view of the milliKelvin cryostat. The instrument is about a meter tall. Not shown is a He compressor and room-temperature readout electronics. A typical HPGe instrument is shown at lower left for comparison. At right is an internal view of the cryostat. The He pulse-tube provides continuous 3.5 K base temperature. A cyclical ADR goes down to 60 mK. The detector array is located at the bottom, surrounded by magnetic shielding. Wire looms and flex cables carry various signals to room-temperature electronics.

readout simultaneously without significant degradation of the energy resolution. The SLEDGEHAMMER instrument under development at the University of Colorado has significantly advanced this technology. The future of microwave SQUID readout looks extremely bright although significant work remains to be done on the room temperature electronics that must generate and demodulate the large number of microwave tones.

The operation of microcalorimeter detectors has cryogenic requirements. A bath temperature on the order of 80 mK is typical. At one time operation at such temperatures would have been considered exotic, but it is routine with modern cryogenic technology. Many cryostat designs exist, each providing certain advantages. Our experiments have utilized a He pulse-tube followed by an adiabatic demagnetization refrigerator (ADR) to reach operating temperature (Figure 3). The He pulse-tube operates continuously and provides a constant base temperature of around 3.5 K. The ADR operates in a cycle where current is applied to the magnet, then drawn down at a rate necessary to maintain the operating temperature. When current has been exhausted, a cycling is required to bring the magnet up to 3.5 K, raise the current, and start the draw down again. No liquid cryogens are used. Sample measurements are limited to the duration of the ADR cycle. With a well-

operating cryostat we achieved measurement times on the order of 24 - 36 hours. Other cryostat technologies could provide much longer measurement times.

An important point is that the sample being measured is outside of the cryostat. There is no need to open the cryostat to measure a new sample. A thin carbon-fiber entrance window separates the internal vacuum of the cryostat from the laboratory environment. Photons with energy greater than a few tens of keV easily pass through the low-density window. The practical low-end of the instrument energy range is around 30 keV. Other instruments have used entrance windows allowing for measurements as low as 200 eV.

The result of a photon striking a microcalorimeter is an electrical pulse whose area and height are proportional to the deposited energy. Simple pulse processing approaches such as picking off the highest point of the pulse or integrating its area fail to use all the information contained in the data and thus do not produce the best resolving power. Under the assumptions that the signal and noise are stationary and that the pulse does not change shape with energy, it can be proven mathematically that the resolving power is maximized by convolving pulses with the optimal filter (Wiener filter) and using the height of the convolved pulses as an uncalibrated energy metric. The optimal filter is constructed from the average pulse shape and the noise power spectral density. Optimal filtering of pulses has been used for over two decades in microcalorimeters [Szymkowiak, 1993].

Many current and potential applications of microcalorimeters involve high photon event rates. In these applications, it is desirable to use piled-up pulses, i.e. pulses that fall on the tail of a previous pulse or that have another pulse in their tail. If these pulses are filtered with the typical optimal filter, the result gives a very poor estimate of the photon energy because the piled-up pulse shape does not match the average pulse shape. As a result, such events must be carefully removed from the data set. Another approach to high rate pulse processing introduced the more general class of filters that are the optimal filter subject to constraints such as orthogonality to constants and orthogonality to exponentials [Alpert, 2013]. This work also used the noise auto covariance instead of the noise power spectral density to construct the optimal filter. With a filter that was orthogonal to both a constant and an exponential decay from a preceding pulse, Alpert et al showed a 45% higher output rate and better resolution for pulses with pile-up. However, the resolution limits are slightly worse for isolated pulses as constraints are added to the filter. Real-time electronic processing of pile-up pulses has also been demonstrated [Tan, 2009].

Finally, we wish to emphasize that microcalorimeter detectors are not an exotic technology operating on the fringe of science. In fact, the core technology has seen successful adaptation to a wide variety of radiation measurements including trace actinide analysis by total decay-energy spectroscopy [Hoover, 2015], x-ray science [Cantor, 2012], astrophysics [Moseley, 1984], and neutrino mass measurements [Croce, 2016].

Key points from this section:

- *Microcalorimeter detectors provide order-of-magnitude improvement in energy resolution for gamma-ray spectroscopy compared to HPGe.*

- *Individual microcalorimeter sensors are small and relatively slow, necessitating the development of large sensor arrays to increase detection efficiency and counting rate.*

- *Microwave multiplexing looks promising for readout of larger arrays of the future.*

- *Offline pulse processing leads to the best resolution performance. Pulse processing methods to deal with high event rates have been developed.*

4. Instrument Performance

The best energy resolution result was achieved using a single pixel exposed to a ^{153}Gd source (gamma-ray lines at 97 and 103 keV). With absorber dimensions 0.95 x 0.95 mm by 0.25 mm thick, a resolution of 22 eV FWHM at 97 keV was achieved [Bacrania, 2009]. This is a factor of 20 improvement over the best HPGe detectors. Subsequently, the quest for higher detection efficiency led to a decision to trade some resolution performance in exchange for a larger absorber mass, and to pursue the development of large sensor arrays where the performance of individual pixels can vary for a variety of reasons. Progress rapidly advanced to a 256-pixel array utilizing 1.5 x 1.5 mm square by 0.38 mm thick absorbers (Figure 4) [Bennett, 2012][Hoover, 2011]. Of the 256 sensors, 239 showed response to biasing, and 236 pixels showed a suitable superconducting transition. Figure 5 shows the measured FWHM energy resolution of the full array using the 97 keV gamma-ray line from ^{153}Gd. The plot shows that 92% of the pixels have an energy resolution lower than 100 eV, and 90% were better than 68 eV. The average energy resolution of the 236 working pixels is 53.3 eV with a standard deviation of 6.9 eV. These measurements were performed at the NIST laboratory where the array was fabricated.

Similar results were achieved after transporting the array to LANL and incorporating it with an equivalent but separate cryostat and readout hardware, where a mean array resolution of 55 eV from a ^{153}Gd source was observed for 226 functional pixels [Winkler, 2015]. A mean resolution of 72 eV was observed from a Pu-oxide sample. The degradation of the resolution for Pu sources is due to periodic disruption of the SQUID multiplexing flux-loop lock when much higher energy photons are absorbed. Recent advances in multiplexing capabilities since the acquisition of these data are expected to obviate this effect.

The 256-pixel array has been demonstrated with a total count rate exceeding 1 kcps, enabled by continuous improvement in the multiplexing hardware and firmware [Winkler, 2015]. A mean array resolution of 72 eV FWHM at 97 keV from a

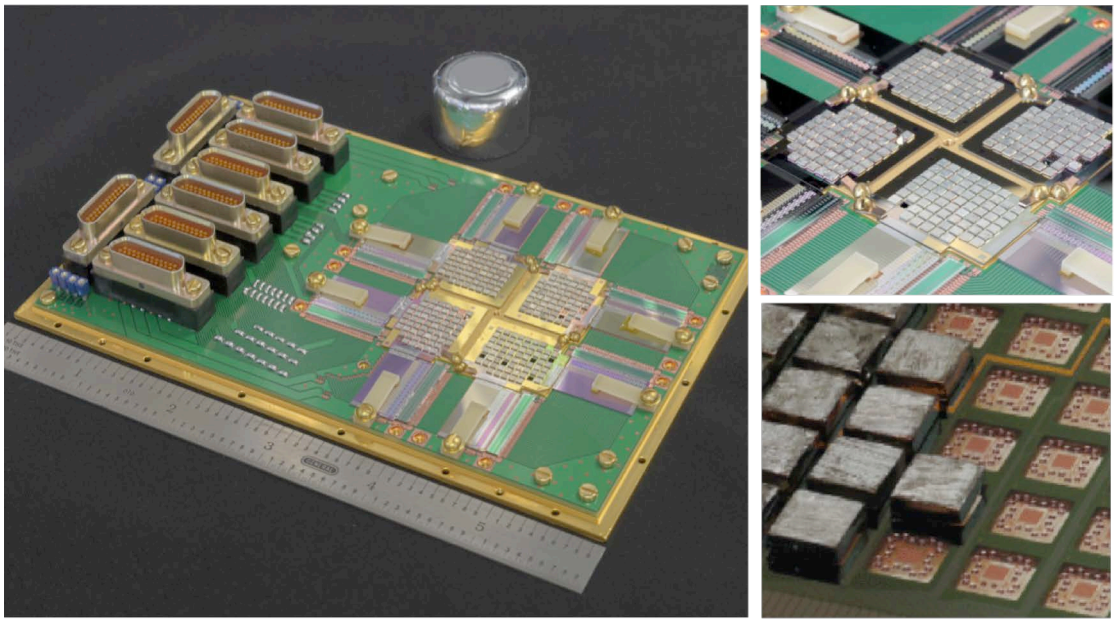

Figure 4 - A 256-pixel microcalorimeter array is shown. At left is the array, composed of four 64-pixel chips, mounted on a PC board with multiplexing interface chips around the edges of the array. A planar HPGe crystal is shown above the array for size comparison. The upper right figure is a closer view of the array and interface multiplexing chips. The lower right figure shows some of the TESs without an absorber attached. The thermally conducting support posts are visible.

^{153}Gd source was measured for a 1.25 kcps total array event rate. The degradation of the energy resolution compared to low event-rate data is caused by thermal and electrical cross-talk between pixels. Small amounts of cross talk can quickly degrade energy resolution when attempting spectroscopy at a part in 1000 resolving power. The layout of certain signal lines on the readout electronics chips was correlated with this effect and newer designs show minimal crosstalk. Mean array resolution for a Pu source at 1.25 kcps was 92 eV FWHM at 103 keV. Again, the resolution degradation for Pu items is a combination of crosstalk and the SQUID lock effect mentioned above.

The detectors have been designed to extend at least up to the 208 keV region, where there are useful peaks for the determination of the isotopic ratios of Pu. In order to characterize the dynamic range and linearity, we mimic gamma-rays using bursts of 1550 nm photons from a pulse-modulated diode laser [Bennett, 2012]. The laser allows for programmable effective pulse energy without all the sources it would take to span the full range of these detectors. The energy response of the TES to the laser can be calibrated against a ^{153}Gd gamma-ray source. The laser is pulsed thousands of times at a given pulse length, and the average current pulse height and pulse area are obtained as a function of laser pulse energy. Figure 6 shows the unfiltered pulse height and pulse area as a function of pulse energy for a single microcalorimeter. Above 400 keV, this detector begins to saturate, and the pulse height is no longer strongly correlated to energy. Information about higher energy pulses can still be obtained from the pulse area, but at a cost of degraded resolution.

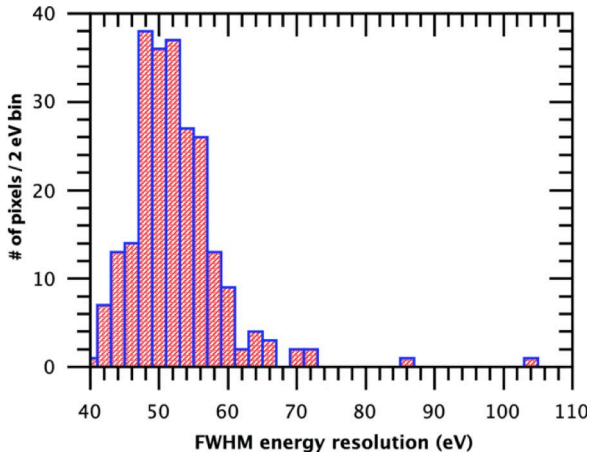

Figure 5 - Measured FWHM energy resolution from 236 microcalorimeter pixels using the 97 keV emission of ^{153}Gd. The average value is 53.3 eV. [Bennett, 2012]

The 256-pixel array provides a total efficiency within a factor of 3 of typical planar HPGe at 100 keV (Figure 7) [Bennett, 2012]. A 1.5 X 1.5 mm square by 0.38 mm thick absorber has a 33 % photopeak efficiency at 100 keV. The upper end of the effective energy range of the instrument presently reaches to about 215 keV, beyond which the stopping power begins to fall off quickly. Certain superconducting materials such as tantalum are, in principle, extremely attractive for x-ray and gamma-ray absorbers. Tantalum has a high atomic number (Z = 73) and a high Debye temperature so that its phononic specific heat is very low. However, detectors using bulk tantalum absorbers show time constants of 10^{-2} s or longer that are largely impractical [Horansky, 2007][Irimatsugawa, 2014]. While these extended time constants may be due to slow thermalization, measurements of the heat capacity of Ta are much higher than the expected phononic contribution, an excess that will slow device recovery [Sellers, 1974]. In contrast, measurements of the heat capacity of Sn are close to the expected values [O'neal, 1965].

Challenges arise when attempting to sum hundreds of individual sensor spectra into a single spectrum for analysis. Spectral summing becomes non-trivial when the energy resolution is high. Issues in energy calibration of the intrinsically non-linear microcalorimeter detectors were described by [Hoteling, 2009]. In a many-pixel array containing detectors with energy resolutions of 80 eV at 100 keV, offsets in the energy calibration of individual spectra as small as 50 eV were shown to produce noticeably distorted peak shapes. Polynomial functions as high as 7th order were found to provide inadequate precision of energy calibration. A cubic spline calibration results in much smaller offsets within 5 eV of the calibration energy [Winkler, 2015]. The summing of data from multiple pixels with different resolutions also introduces additional non-Gaussian peak shape distortions in the final summed spectrum. Recent advances in multiplexing hardware allowing for

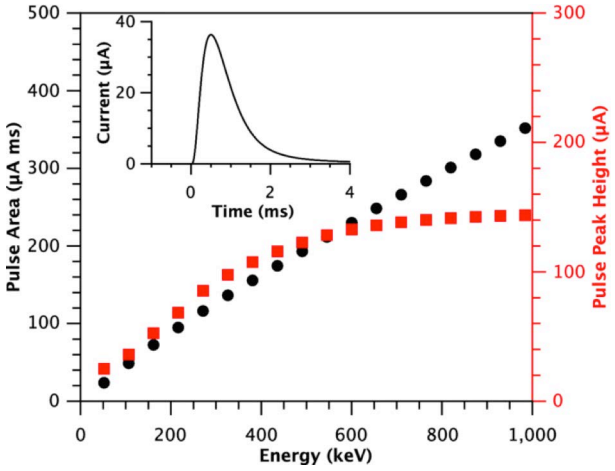

Figure 6 - A measurement of detector response linearity using a laser pulser. The response begins to saturate above 400 keV. The inset shows typical pulse response to 103 keV gamma-ray. [Bennett, 2012]

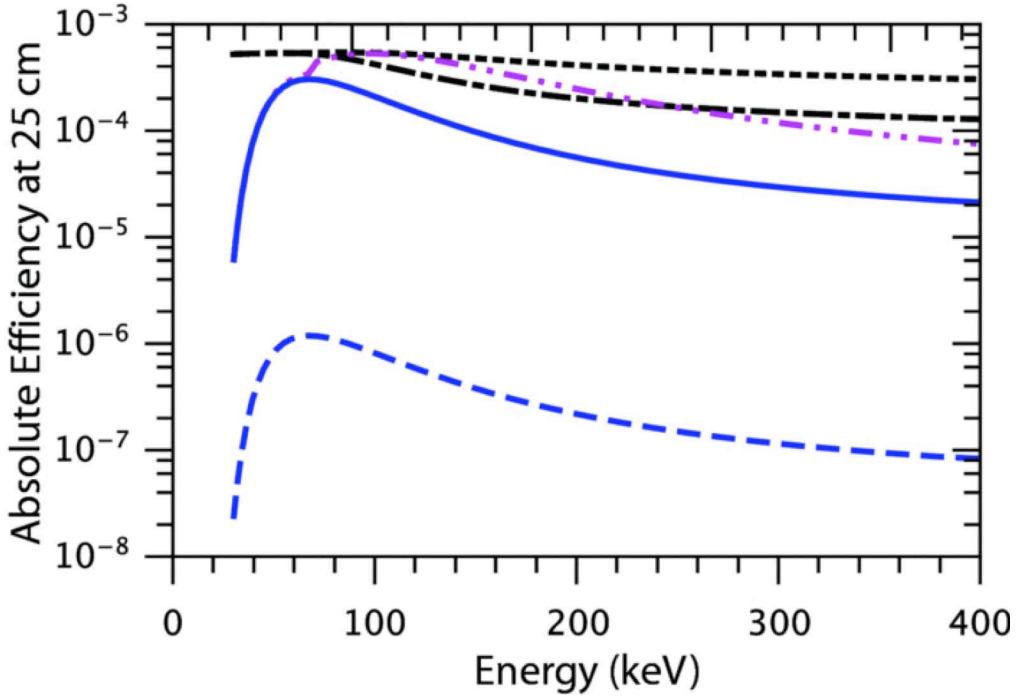

Figure 7 - Estimated absolute efficiency at 25 cm for single pixel microcalorimeter detector (blue dash), 256-pixel microcalorimeter array (blue solid), and 256-pixel array with Ta absorbers (magenta dash-dot-dot). Also shown are 2.5 cm diameter by 0.5 cm thick (black dash-dot) and 1.5 cm thick (black dash) HPGe detector. [Bennett, 2012]

better tuning of operational SQUID parameters is expected to significantly improve performance uniformity across the array. Time-dependent gain drift can be observed during data acquisition. While a correction is applied for this effect, it is imperfect over the ~20 hour integrations commonly used so far, and sometimes leads to additional distortion of the spectral peak shapes. The combination of these effects becomes important when performing quantitative spectral analysis. A different possible overall approach is to analyze the individual spectra, then combine the results. This should be statistically equivalent to analyzing the summed spectrum, but requires enough counts in the individual pixel spectra to be viable.

Data from Pu samples have been collected throughout the research and development process, from the first single-pixel device to the most recent 256-pixel array. The first single-pixel spectrum had thousands of counts, while the most recent array spectra have tens of millions of counts [Ullom, 2005][Winkler, 2015]. High-quality spectral data suitable for quantitative analysis were collected from reference standards with well-established isotopic compositions (see Table 1). Specifically, we obtained data from: PIDIE samples 1, 3, 6; CBNM samples 61, 70, 84, 93; and FZC-158 [Hoover, 2014][Winkler, 2015]. The mass of these samples ranges from 0.4 for the PIDIE series, 5.5 g for the CBNM series, and 0.7 g for FZC-158.

Figure 8 shows the PIDIE-3 sample 100 keV region measured with a microcalorimeter array and a planar HPGe detector. The greatly improved resolution and separation of spectral peaks in the microcalorimeter data are obvious. Figure 9 shows measured spectra from all the PIDIE samples, CBNM samples, and FZC-158. We have also collected data from other items including a

Table 1 – Summary of Pu calibrated standard sources used for quantitative analysis, ordered by ^{240}Pu content. Values from MS analysis (except FZC-158 where values determined from HPGe are shown due to limited available MS data). The samples span a significant range of isotopic compositions. All sources are Pu-oxide form sealed in metal canisters. Total Pu mass is 0.4 g for PIDIE samples, 5.5 g for CBNM samples, and 0.7 g for FZC-158.

Sample	^{238}Pu/Pu	^{239}Pu/Pu	^{240}Pu/Pu	^{241}Pu/Pu	^{241}Am/Pu
PIDIE-1	0.0093	94	5.9	0.068	0.35
CBNM-93	0.0095	94	6.3	0.061	0.26
PIDIE-3	0.04	85	14	0.34	1.2
CBNM-84	0.057	85	14	0.28	0.96
CBNM-70	0.71	76	19	1.5	5.3
PIDIE-6	0.81	69	25	1.9	7.3
CBNM-61	1.0	66	27	2.1	6.3
FZC-158	0.012	0.96	94	0.13	0.56

MOX surrogate material, highly-enriched uranium [Hoover, 2009], and combined ^{235}U/^{226}Ra sources (Figure 10) [Hoover, 2009]. In all, the data collected from the PIDIE, CBNM, and FZC-158 sources represent approximately 1300 hours of integrated measurement time. This collective data set obtained over a number of years provides the foundation on which to begin examination of spectral analysis methods and assess the performance of microcalorimeters for quantitative isotopic analysis.

Key points from this section:

- *The best microcalorimeter energy resolution achieved was 22 eV FWHM at 97 keV, a factor of 20 better than HPGe. A tradeoff exists between absorber size and resolution.*

- *Simultaneous readout of a 256-pixel array has been demonstrated using time-domain multiplexing. Mean energy resolution is in the range of 50 - 60 eV FWHM.*

- *Total array counting rates exceeding 1 kcps were demonstrated. Some degradation of resolution was observed for high count rates and sources with high photon energies due to pixel crosstalk and operating near the limits of the multiplexing hardware available at the time.*

- *Spectra on reference Pu samples with tens of millions of counts have been collected and form the basis of studies on quantitative analysis and measurement uncertainty.*

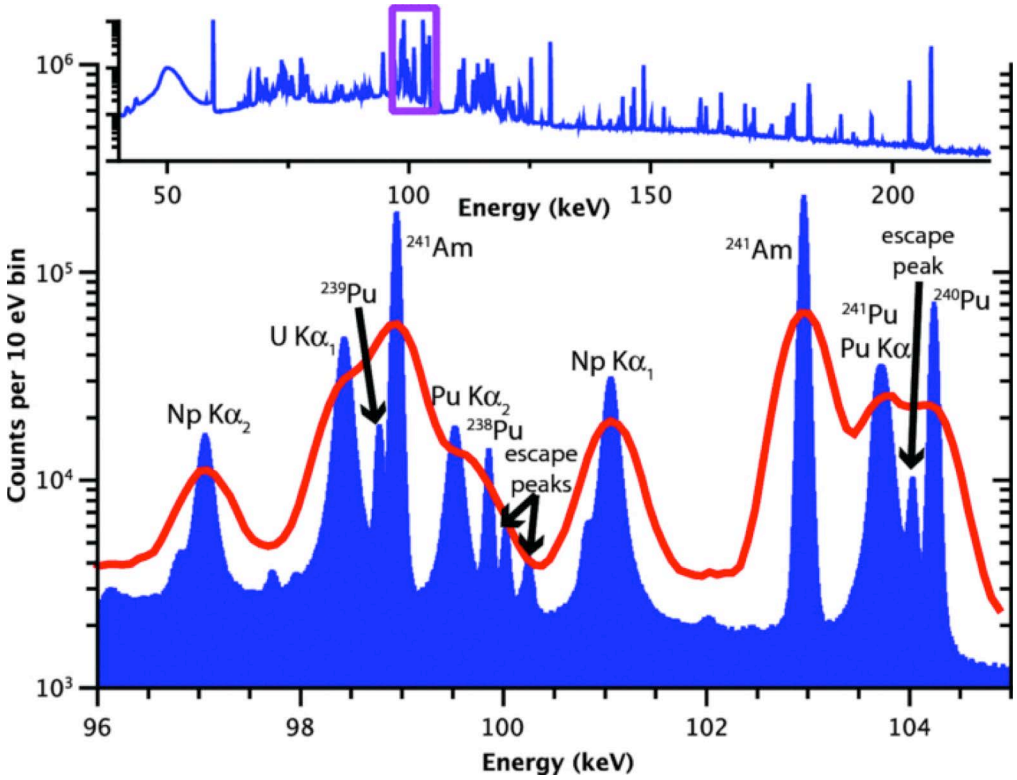

Figure 8 - Measured spectrum from PIDIE-3 sample comparing microcalorimeter data (blue) and HPGe (red). The inset shows the same spectrum over a wider energy range from 40 – 220 keV. Note greatly improved peak resolution of the microcalorimeter data, and x-ray Lorentzian line shapes visible by eye. [Bennett, 2012]

5. Quantitative Analysis

The collection of spectra with millions of counts from Pu reference standards having well-documented isotopic composition enabled us to undertake a study of the improvement provided by the higher energy resolution. Initially the work focused on statistical (or random) uncertainty [Hoover, 2013]. This was later expanded to include systematic uncertainties [Hoover, 2014]. As is clearly evident in Figure 8, the 100 keV region of Pu samples is dense with gamma-ray lines. Even with HPGe resolution the individual photopeaks are not well-resolved. The microcalorimeter data, in contrast, provide much better peak resolution. By reducing or removing peak overlaps and improving signal to background, the measurement uncertainties of extracted above-background peak areas are reduced. This is expected to translate into improved precision and accuracy in the isotopic content values determined from the spectral analysis.

Initially, we employed existing analysis codes developed for HPGe data [Karpius, 2009][Lee, 2011]. The FRAM code, for example, is widely used in the safeguards world for HPGe spectral analysis [Sampson, 1989]. However, we uncovered a number of desired modifications that could best be addressed by developing a new analysis code platform. Key differences from existing codes like FRAM are the use of more free parameters during peak fitting, a new peak shape for

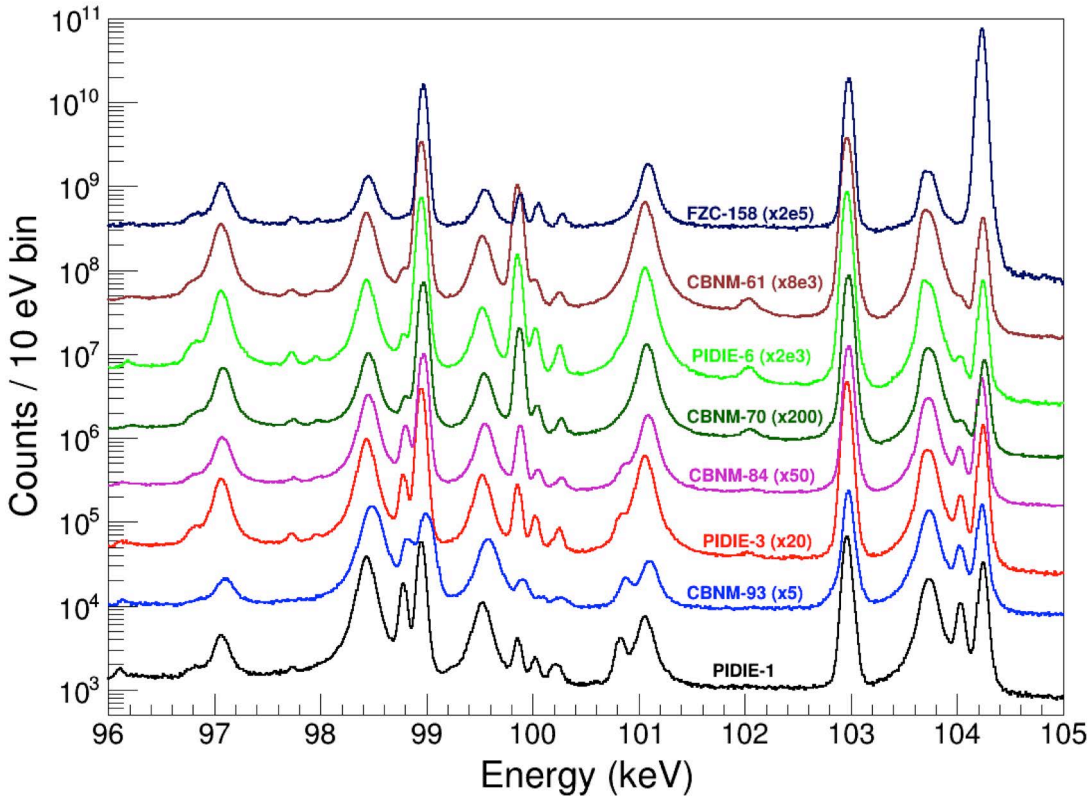

Figure 9 - An overlay comparing measured microcalorimeter data collected from the Pu isotopic standards in Table 1. For visual clarity the spectra have been scaled as indicated. See Figure 8 for identification of spectral peaks. Total collected counts for these spectra in the 96 – 210 keV energy region range from 8.2e6 to 3.7e7.

microcalorimeter data, and the ability to include uncertainties in tabulated branching fractions and isotope half-lives. Some differences exist in the computation of statistical errors for isotopic ratios. In order to ensure a direct comparison with equal treatment of the data, the code is able to analyze HPGe as well as microcalorimeter data.

The first stage of analysis is the fitting of spectral peaks to extract above-background peak areas. For HPGe data, we use a Gaussian photopeak with a low-energy exponential tail for the peak model. The fundamental peak shape measured by each microcalorimeter pixel is expected to be Gaussian. As discussed above, the spread of energy resolutions and small calibration variations for each pixel result in deviations from a Gaussian peak shape when the data from many pixels are summed into a spectrum. We model the resulting combined microcalorimeter peak shape as a sum of two Gaussians with identical centroid energies and different widths. The background under the photopeak is modeled as a simple flat step-function, broadened by the detector resolution. The natural Lorentzian shape of the x-ray peaks, combined with the detector resolution, is modeled with a pseudo-Voigt function [Thompson, 1987]. X-ray line widths are fixed to the values in [Krause, 1979].

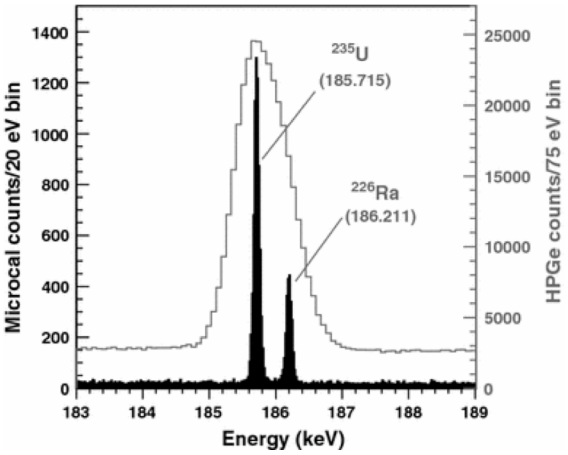

Figure 10 - A simultaneous measurement of the 185.715 keV line of ^{235}U (primary line for U enrichment determination) and the 186.211 keV line of ^{226}Ra (ubiquitous naturally-occurring background). The peaks are easily resolved with a microcalorimeter (black data). HPGe resolution is inadequate for any level of separation (gray data). [Hoover, 2009]

Peak fitting occurs within user-defined energy regions-of-interest (ROIs). In the dense 100 keV region, even though there is much less peak overlap in the microcalorimeter data, it is still problematic to find clean regions to define backgrounds for peak fitting. Thus, the 100 keV region is fit as one large ROI containing many peaks. Compared to existing methods (e.g. - FRAM), we allow more parameters to float during peak fitting, though there are necessary differences in the treatment of HPGe and microcalorimeter data. For HPGe spectra, we simultaneously float the peak amplitudes, the tail amplitude, a global peak width, and an energy calibration adjustment parameter. Importantly (as will become evident in subsequent discussion of systematic uncertainty), the improved peak separation in the microcalorimeter spectra permit us to have the energy centroid for each peak be a free parameter, overcoming offsets in energy calibration or uncertainties in tabulated gamma-ray energies. These additional degrees of freedom come with a cost of increased difficulty for the minimization routine. To fit the 100 keV region of a microcalorimeter spectrum requires simultaneous minimization of 38 free parameters. This might seem intractable, but one can deduce reasonable starting values and limits for most parameters, resulting in convergence of the minimization routine in most cases.

Two examples of peak fitting are shown in Figures 11 and 12, where the spectral regions containing ^{240}Pu gamma-rays at 104.23 keV and 160.31 keV are shown. In Figure 11, notice the considerable peak overlap in the HPGe data of the 104.23 keV peak and the Pu Kα_1 x-ray at 103.73 keV. The microcalorimeter detector is able to significantly decrease peak overlap in this region. Two small, additional peaks occur in the microcalorimeter spectrum at 104.025 keV and 104.252 keV that are not in the HPGe data. These are tin escape peaks, produced when a photon interaction generates a tin x-ray that subsequently escapes the absorber instead of being absorbed. This phenomenon is unfortunate, as the appearance of the escape peaks complicates the microcalorimeter spectrum, working against the benefit of increased resolution. The 160.31 keV peak is especially difficult for HPGe to resolve given the 353 eV separation from the 159.95 keV line of ^{241}Pu. For these lines, the superior resolving power of the microcalorimeter detector is clear, achieving nearly complete peak separation (Figure 12).

Uncertainties of the above background peak areas are returned from the fitting routine. To isolate the effect of improved energy resolution, the microcalorimeter and HPGe results are compared assuming an equal number of

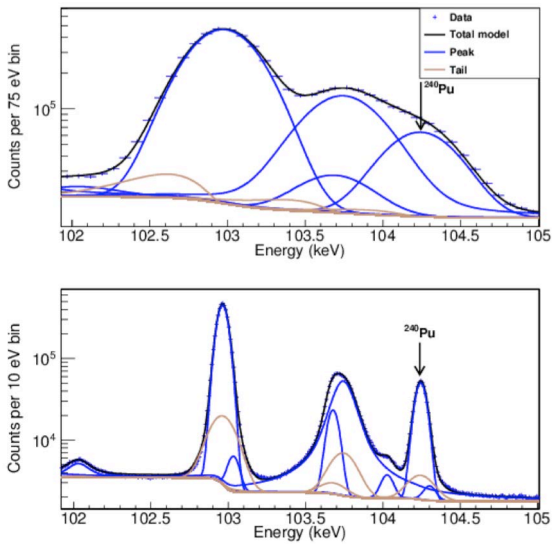

Figure 11 - Spectral region surrounding the 104.23 keV ^{240}Pu peak measured with HPGe (top) and microcalorimeter (bottom). [Hoover, 2013]

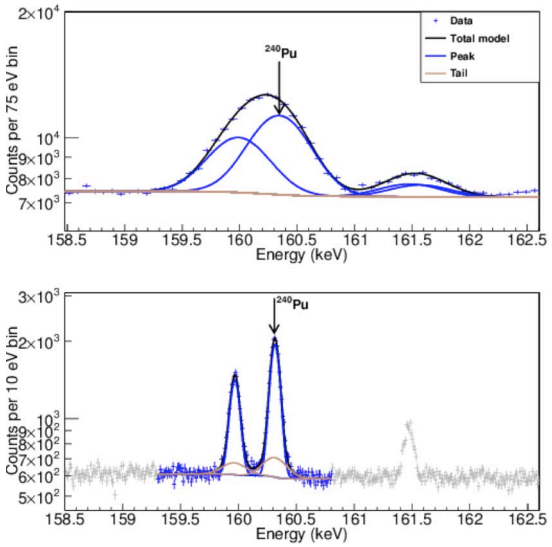

Figure 12 - Spectral region surrounding the 160.31 keV ^{240}Pu peak measured with HPGe (top) and microcalorimeter (bottom). [Hoover, 2013]

counts in the photopeak. Presently, HPGe detectors can collect counts at a much higher rate than the microcalorimeter array, but advances in array size and counting rates will close this gap in the future. For equal total photopeak counts, analysis of the microcalorimeter data results in a factor of 2.2 lower uncertainty compared to the HPGe data for the 140.23 keV peak, and a factor of 6.4 lower uncertainty for the 160.31 keV peak. These are just two examples. Some peaks, such as the ^{239}Pu 129 keV peak and ^{241}Pu/^{241}Am 208 keV peak are isolated, relatively strong, and do not benefit significantly from improved energy resolution. The potential improvement of the microcalorimeter detector for isotopic ratio measurements is a combined effect averaged over many peaks with differing levels of overlap and signal to background level that varies with isotopic composition. Thus, an order of magnitude improvement in energy resolution does not directly translate to equal improvement in the extracted peak area uncertainties.

The peak areas and their errors are subsequently used to determine the isotopic composition. For each gamma-ray line, the peak area is divided by the branching ratio and the data are simultaneously fit to a source-detector efficiency curve of the form

$$\frac{Peak\ Area}{Branching\ Fraction} = \frac{(1 - e^{-\mu_{Pu}\rho_{Pu}x_{Pu}})}{\mu_{Pu}\rho_{Pu}x_{Pu}} e^{-\mu_{Cd}\rho_{Cd}x_{Cd}} I_i E^b c^{1/E} \qquad (1)$$

This form of the relative efficiency curve is the same as that used by the FRAM code [Sampson, 2003]. The first term on the right-hand side describes the attenuation in the plutonium source. The second term accounts for attenuation in cadmium shielding that is used to knock-down the intensity of the ^{241}Am 60 keV line. The I_i are the intensities of the isotopes ^{238}Pu, ^{240}Pu, ^{241}Pu, and ^{241}Am relative to ^{239}Pu. The final term is the detector relative efficiency. The fit requires simultaneous

Table 2 – Summary of improvement in statistical uncertainty for Pu isotope ratios using microcalorimeter data versus HPGe data. Values are the microcalorimeter isotope ratio uncertainty divided by the HPGe uncertainty. The inverse (HPGe divided by microcalorimeter) is shown in parentheses. Results were normalized by total counts in the 96 – 210 keV region. Some values > 1 result from this normalization and the lower detection efficiency of the microcalorimeter compared to HPGe for the $^{241}Am/^{241}Pu$ 208 keV line. The greatest improvement occurs for the low-burnup samples.

Sample	$^{238}Pu/^{239}Pu$	$^{240}Pu/^{239}Pu$	$^{241}Pu/^{239}Pu$	$^{241}Am/^{239}Pu$
PIDIE-1	0.19 (5.3)	0.20 (5.0)	1.0 (1.0)	0.32 (3.1)
CBNM-93	0.22 (4.5)	0.60 (1.7)	1.1 (0.91)	0.22 (4.5)
PIDIE-3	0.29 (3.4)	0.47 (2.1)	1.1 (0.91)	0.52 (1.9)
CBNM-84	0.27 (3.7)	0.49 (2.0)	1.1 (0.91)	0.71 (1.4)
CBNM-70	0.77 (1.3)	0.28 (3.6)	1.1 (0.91)	0.91 (1.1)
PIDIE-6	0.79 (1.3)	0.70 (1.4)	1.1 (0.91)	1.0 (1.0)
CBNM-61	0.86 (1.2)	0.46 (2.2)	1.0 (1.0)	0.8 (1.2)
FZC-158	0.61 (1.6)	0.77 (1.3)	0.83 (1.2)	0.75 (1.3)

minimization of 9 free parameters using 15 peak areas. The minimization routine outputs the intensities of the isotopes and their errors. Isotope specific activities are used to convert these to mass percents.

Measurements of several Pu isotopic standards (PIDIE-1,3,5; CBNM-61,70,93; FZC-158) having a range of isotopic compositions (see Table 1) were used to determine the improvement in statistical uncertainty of extracted isotope mass ratios when using microcalorimeter data compared to HPGe. The analysis utilized photopeaks in the range of 96 keV to 210 keV. For purposes of comparison we report results assuming the same total number of counts in this energy range for microcalorimeter and HPGe spectra (Table 2). The most significant improvement is observed for the $^{238}Pu/^{239}Pu$ ratio of the PIDIE-1 sample, where the microcalorimeter provides a factor of 5.3 improvement over HPGe. The improvement provided by the microcalorimeter data generally increases as the material enrichment decreases (PIDIE-1 results show a larger improvement than PIDIE-6, for example). There is minimal improvement for the $^{241}Pu/^{239}Pu$ ratio, due to the fact that the primary gamma-ray peaks for these isotopes (129 keV, 208 keV) are strong and isolated. The FZC-158 results are more uniform across the isotope ratios, since the very low ^{239}Pu content becomes a limiting factor in the ratios.

The values in Table 2 provide an indication of the improvement in statistical error when using the microcalorimeter array, but likely underestimate the true improvement because the different detector resolutions require differences in the peak fitting algorithms. The HPGe data were fit with fewer free parameters (in particular a number of gamma-ray energies are fixed), which reduces the statistical error. A completely fair comparison would require the HPGe peak fitting to have all peak energies be free parameters as is done for the microcalorimeter data, but this is not practically achievable.

Using the uncertainty derivations of [Sampson, 1983], a factor of 4.7 improvement in the relative statistical uncertainty of the sample specific power is predicted for the PIDIE-1 sample if the microcalorimeter data are used. The total Pu mass statistical uncertainty would be improved by the same amount, assuming a perfect measurement of the total sample activity. Note the improvement is strongly dependent on burnup. A similar analysis for the PIDIE-6 sample predicts only a factor of 1.1 improvement in relative statistical error for the sample specific power.

For the extraction of above background peak areas, the improvement is highly dependent on the degree of peak overlap, relative strength of overlapping peaks, and peak-to-background ratio. The improvement may range from a factor of nearly ten, to zero. The extraction of isotope ratios combines all the peak areas in the source-detector efficiency curve fit, so the net improvement is really an average across many peaks, and improvement as large as a factor of 5 has been observed. Calculation of specific power involves additional mathematics that combines the isotope ratio uncertainties. The most significant improvements are observed for the low-burnup samples, which is intuitive because the non-^{239}Pu gamma-ray lines will be weaker in these cases.

The discussion of statistical uncertainty is interesting and important, but the ultimate uncertainty limits are governed by systematic uncertainties. The accumulation of spectra with an increasingly large number of total counts can be easily realized with multiple detectors and longer counting times. Statistical uncertainty can be driven to an arbitrarily small value simply by collecting more counts. Operation of an HPGe detector for a few hours is usually sufficient to lower the statistical uncertainty to a level below the dominant systematic uncertainties. Assuming that achievable microcalorimeter counting rates will continue to increase with the development of larger sensor arrays, the best achievable total measurement uncertainty is dependent on these limiting systematic errors.

Upon examining the measurement results, it became evident that the accuracy of the isotope ratios using the microcalorimeter data was similar to that from HPGe data, on the order of 1 - 2 %, despite reported peak area statistical uncertainties well below 1 % (Figure 13). Throughout the above discussion of statistical uncertainty, note that a number of material properties and nuclear data are required for the complete analysis. Peak fitting uses x-ray line widths and x-ray and gamma-ray line energies. Determining the isotope ratios requires attenuation coefficients, material densities, branching ratios, and half-lives. We utilized models to describe spectral peak shapes and backgrounds. We also invoked a source-detector efficiency curve to model the system being measured, and the detector performing the measurement. The final determination of isotope ratios is therefor

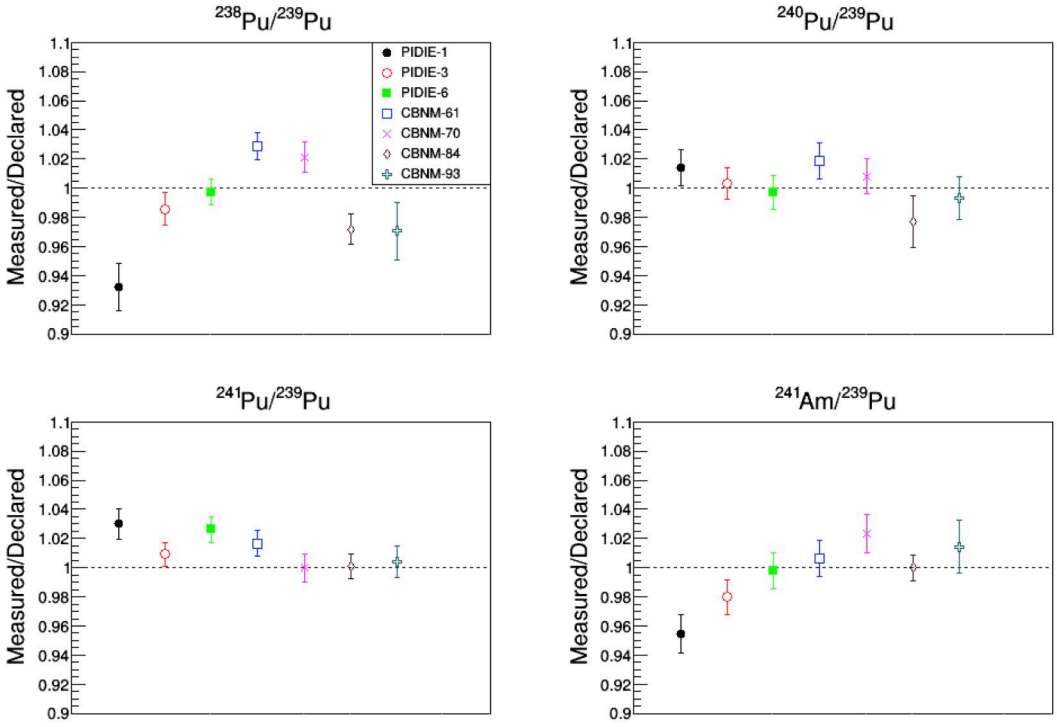

Figure 13 - Summary of microcalorimeter isotopic ratio measurements from the Pu standards. The measured value divided by the known value (from MS analysis) is plotted. Sample and isotope dependent errors on the order of a few percent are observed. Error bars include counting statistics, gamma-ray branching fraction uncertainty, and isotope half-life uncertainty.

dependent on a number of quantities that are insensitive to any improvement of peak area statistical uncertainty. How well do our models describe the actual data? How well are the required external parameters known? The collection of more counts or improvement of energy resolution will not reduce the uncertainty of these quantities.

X-ray and gamma-ray energy uncertainties are on the order of tens of eV or less (0.001 - 0.3 % relative error) [Deslattes, 2003][Qaim, 1992]. Gamma-ray branching fraction uncertainties are on the order of 0.5 – 4 % for the line energies of interest to this analysis [Qaim, 1992]. Isotope half-life uncertainties range from 0.04 - 0.14 % for the Pu and Am isotopes considered [Qaim, 1992]. X-ray line width uncertainty is on the order of 4 % [Krause, 1979]. Mass attenuation coefficient uncertainty is on the order of 2 % [Hubbell, 1982][Trubey, 1989][Rettschlag, 2007]. Uncertainty of the relative emission rate of tin X-rays is about 2 % [Salem, 1974]. The variability in the densities of materials relevant to this measurement (plutonium, cadmium-shielding, etc.) is not well-understood, so we will assume a 1 % uncertainty for this discussion.

For two of the parameters of interest, gamma-ray branching fractions and isotope half-lives, the uncertainties can be evaluated for each spectral analysis by simple mathematical calculation. As evident from the left side of Equation 1, the uncertainty of each gamma-ray branching fraction can simply be combined in

quadrature with the corresponding peak area uncertainty. Likewise, when the isotope ratios from the efficiency curve fit are multiplied by the half-lives to convert activity ratios to mass ratios, the half-life uncertainties can be combined in quadrature with the isotope intensity uncertainties. Uncertainties in gamma-ray branching fractions and isotope half-lives are applied after spectral peak fitting has occurred, and their effects are the same for the HPGe and microcalorimeter analyses. The relative uncertainty from branching fractions ranges from 0.8 to 1.2 %. For the isotope half-lives, the uncertainty is considerably smaller, about 0.15% on average.

The remaining constants of nature are more difficult to assess, because one or two fitting routines (peak fitting and efficiency curve fitting) must be executed to determine the effect of their uncertainties, precluding simple mathematical propagation. For these we determine the sensitivity coefficient by applying random adjustments to the constants of nature and observing the resulting change in isotopic ratios. Through many trials, each having a unique random adjustment, we can quantify the effects.

The effect of x-ray line widths varies. For HPGe analysis the effect is typically in the range 0.1 to 0.8 % For the microcalorimeter analysis it is nearly always at or below 0.1%. We find very little sensitivity of the isotopic ratios to the uncertainty in the mass attenuation coefficients and material densities. Both produce variation in isotopic ratios less than 0.001 % relative uncertainty. This is perhaps not unexpected, as we are computing isotope ratios rather than absolute intensities. If the attenuation or density is changed, the isotope intensities can be changed to counter the effect, leaving the isotope ratios unchanged. We also find a small effect from the tin x-ray relative emission intensities, producing less than 0.03 % variation in isotope ratios for the microcalorimeter analysis.

A notable difference appears for the effect of uncertainties in gamma-ray energies. The energy uncertainties produce much larger errors in HPGe data than in microcalorimeter data since the worse resolution of HPGe does not allow all the line positions to be adjusted while fitting. The microcalorimeter peak fit routine can adjust the gamma-ray energies to obtain the best match to the data, meaning the final result is largely insensitive to the starting energies. The uncertainties from gamma-ray line energies for HPGe analysis are in the range 0.2 – 3 %, while for microcalorimeter data the effect is generally below 0.05 %.

Table 3 summarizes the approximate order of magnitude uncertainty for each effect. A detailed accounting of these values across isotope ratios and sample composition is available in [Hoover, 2014]. A key point is evident from the data. Microcalorimeter results are dominated by uncertainties in branching fractions at the level of one percent. If the uncertainties of branching fractions could be significantly reduced, the total uncertainty from constants of nature for the microcalorimeter would fall from the percent level to the tenths-of-percent level. For HPGe, however, the significant factor of gamma-ray energies would still limit the total uncertainty to the percent level. As the uncertainties on gamma-ray energies are already quite low (<0.24 %), reducing this limiting factor would appear unlikely. If other sources of systematic error can be reduced so that the uncertainties caused by constants of nature become the dominant factor, and if experimentation can

Table 3 – The uncertainty (in %) associated with several constants of nature for analysis of Pu isotope ratios with HPGe and microcalorimeter data. Data for the PIDIE samples are shown, which span a range of material burnup. Values are a range over the four isotope ratios with respect to ^{239}Pu. Gamma-ray branching fractions and isotope half-lives are used independently of spectral peak fitting and have equal effects for HPGe and microcalorimeter. Note that the very small uncertainties in gamma-ray energies produce large uncertainties in the HPGe analysis, but much smaller uncertainties in the microcalorimeter analysis (red highlight). [Hoover, 2014]

HPGe			
Parameter	***PIDIE-1***	***PIDIE-3***	***PIDIE-6***
Branching Fraction (σ=0.5-3.8%)	0.8 – 1.2	0.8 – 1.2	0.8 – 1.2
Half Life (σ=0.04-0.14%)	0.1 – 0.2	0.1 – 0.2	0.1 – 0.2
Energy (σ=0.0007-0.24%)	1.1 – 3.1	0.7 – 1.4	0.2 - 1.0
x-ray line width (σ=4%)	0.3 – 1.0	0.04 – 0.8	0.25 -0.35

Microcalorimeter			
Parameter	***PIDIE-1***	***PIDIE-3***	***PIDIE-6***
Branching Fraction (σ=0.5-3.8%)	0.8 – 1.2	0.8 – 1.2	0.8 – 1.2
Half Life (σ=0.04-0.14%)	0.1 – 0.2	0.1 – 0.2	0.1 – 0.2
Energy (σ=0.0007-0.24%)	0.05 – 0.15	0.01 - 0.04	0.02 – 0.05
x-ray line width (σ=4%)	0.04 – 0.6	0.04 – 0.15	0.01 – 0.02

reduce the uncertainty on branching fractions, the lowest achievable uncertainty of the microcalorimeter would be a factor of ten below HPGe.

A few general ideas about how to approach the constants of nature problem have been identified, but not detailed thoroughly. New measurements of x-ray line widths may be the most accessible. The resolution of HPGe (~500 eV) is 5 times larger than the Pu line widths (~100 eV). The resolution of a microcalorimeter can be as good as ~20 eV, a factor of 5 smaller than the line widths, making the measurement more sensitive to the true peak shape. Measurements of absolute gamma-ray branching fractions are hard, and we assume that great effort has been expended to assemble the presently available data. Nevertheless, improved data would be highly valuable for the reason outlined above, and we think investment in this area of nuclear data should be pursued.

An alternative approach used in the FRAM code is to treat branching fractions as calibration parameters whose best values are determined through analysis of data from many samples [Burr, 2005], which could prove more tractable than attempts to reduce tabulated uncertainties of branching fractions. Adjustment

of the branching fractions might reduce the overall systematic uncertainty of analysis results, but would require a large library of measured spectra from a variety of items. This approach could be interpreted by some as the application of ad hoc correction factors, thereby reducing the perceived level of scientific rigor.

Finally, there is the idea of reformulating the problem. In some cases, the ratio of two values can be known with much greater precision than either of the two values themselves. Consider the fine structure constant alpha, known to 0.2 ppb, even though the electron charge is known to only 6 ppb, and Planck's constant to 12 ppb. Perhaps the spectral analysis problem could be reformulated in terms of ratios of branching fractions, or other combinations of factors, in a way that would lower the uncertainty limits. This idea also requires further investigation.

Less is known about systematic uncertainty introduced by models of the spectral peak shape and source-detector efficiency curve models. We know that in both cases, as the total number of counts grows (and the statistical error bars shrink), goodness of fit parameters like reduced chi-squared also grow, indicating a discrepancy. To improve on HPGe analysis these models will need to be accurate to better than 1 %. The peak shape model accuracy will improve as the gain and resolution performance of all the sensors in the array becomes more uniform. This is likely given improvements in fabrication methods, increase in the multiplexing sample rate, reduction of crosstalk, and utilization of automated SQUID parameter tuning software. The source-detector efficiency curve model has a number of assumptions. It assumes slab source geometry for the self absorption term. Only a few intervening material terms can be used before minimization of the fit becomes problematic. The detector efficiency is determined from the data. Even if the detector efficiency were measured separately, could it ever be measured with a sub-percent level of uncertainty? Even if all constants of nature were known exactly, the accuracy with which these models can match the measured data would still present an uncertainty limit that might preclude reaching the target total uncertainty level. More work is required on this topic as well.

The use of simulations may have an important role in understanding the systematic errors. The generation of synthetic spectra could provide "perfect" data on which to exercise the spectral analysis methods. Anomalies in peak shapes, detector response, source absorption, and constants of nature could be applied at will to observe the effect of model discrepancy on peak fitting and isotopic analysis. Some work was pursued in this area using a Monte Carlo approach to achieve the highest fidelity in background continuum, detector response, and x-ray signals [Hoover, 2007][Hoover, 2009c]. A lower-fidelity but more practical analytical model could likely be developed to provide simulated spectra much faster and with much easier control over the relevant parameters.

<u>Key points from this section:</u>

- *The study of total measurement uncertainty was enabled in recent years by the collection of data sets with tens of millions of counts from samples with a range of isotopics*

- *Order of magnitude improvement in energy resolution does not directly translate to the same level of improvement in statistical uncertainty of extracted peak areas and isotope ratios. Peak area uncertainty is highly dependent on the level of overlap, relative strength, and signal-to-background level. Isotope ratio uncertainty is an average effect combining data from multiple spectral peaks. In some cases the microcalorimeter data provide significant reduction of statistical uncertainty. In other cases the improvement is minimal.*

- *The true limiting factor is systematic uncertainty. The microcalorimeter analysis is primarily limited by gamma-ray branching fractions. Improved nuclear data or reformulation of the problem could reduce the theoretical uncertainty limit from constants of nature to well below 1%. HPGe analysis would still be limited to the 1% level by the uncertainty of gamma-ray line energies.*

- *The effect of model discrepancy is perhaps the least well-understood contribution to the total measurement uncertainty. Model discrepancy is the difference between spectral peak shape models, source-detector efficiency model, and the real data.*

6. Implementation at nuclear facilities

To date, research and development has occurred within the comfortable confines of our laboratories at NIST and LANL. The necessary next step is to move beyond the home laboratory into real-world environments like reprocessing plants, MOX production plants, and other large nuclear facilities. The central goal of our work is to enable Near Real-Time Analysis (NRTA) via improved x-ray and gamma-ray spectroscopy with uncertainty limits approaching those of traditional DA techniques.

The scope of the analytical task posed by safeguarding a large facility bears mention. Safeguards at Rokkasho (and the much smaller Tokai plant) are estimated to consume 20% of the IAEA's annual safeguards budget [Johnson, 2009]. Further, *"There are a very large number of safeguards samples and it is still difficult to obtain sample results in a timely manner – even with the On-Site Laboratory."* [Durst, 2007] Clearly, there is a need for accurate NDA technologies capable of rapid, low-cost analysis.

These technologies will have an additional benefit: improved process control at U.S. nuclear facilities. The F/H-Canyon analytical laboratory at Savannah River Site supports H-Canyon operations by performing as many as 6,000 MS analyses a year for process control. The turnaround time for an analysis is 36-48 hrs. If high precision compositional measurements can be performed with gamma–ray spectroscopy in about 30 minutes, more process data can be obtained more quickly and with less effort. Further, MS measurements at the accountability sample points are so critical that they must be completed before the solution moves forward in the

process. Faster analysis of material from these plant locations will directly increase plant throughput. We make the general observation that gamma-ray spectroscopy is not well matched to measurements inside an actual reprocessing canyon; the radiation levels are high and any spectrometer is at risk of costly contamination. Fortunately, nuclear facilities are routinely instrumented with large numbers of sampling points for process control and safeguards.

Within the context of a PUREX reprocessing stream, several opportunities exist to apply the microcalorimeter technology:

- Spent fuel is received at the plant and dissolved. Determining the Pu content of spent fuel is a safeguards grail because burn-up calculations of Pu content provided by the operator can have uncertainties of 10 % or more [Johnson, 2009]. However, determining Pu content is extremely challenging because of the complex geometry of fuel assemblies and the high radiation fields from fission products. Our team has conducted measurements (using HPGe detectors) and simulations that suggest the Pu content (elemental, not isotopic) of spent fuel can be measured from self-induced U and Pu x-ray fluorescence lines and knowledge of the initial U content of the fuel [Hoover, 2009b]. Even with the fission product background, it may be possible to obtain information about total Pu content using microcalorimeter detectors, which provide better signal-to-background ratio in the 100 keV x-ray region.

- U and Pu are separated from each other and from fission products and other actinides. These purified streams are ideally suited to analysis using a microcalorimeter gamma-ray spectrometer. Separated material is analyzed for total Pu, Pu isotopics and metal contamination using mass-spectrometry. Since the fission products have been removed by this point, the same information could potentially be obtained much more quickly using a microcalorimeter detector.

- Waste material is prepared for disposal. There are multiple types of waste. Some are mixed together, liquid wastes are typically concentrated by evaporation, and most waste is vitrified before containment in canisters. Current safeguards measurements rely on mass spectrometry to establish the Cm/Pu/U ratio combined with neutron measurements (which are dominated by ^{244}Cm) to infer the Pu quantity [Johnson, 2010]. In the future, microcalorimeters may be able to establish the Cm/Pu/U ratio nondestructively using self-induced x-ray fluorescence. While separations waste containing fission products may be challenging to measure, waste from oxide powder production does not contain fission products and is already analyzed "semi-quantitatively" using HPGe spectroscopy [Johnson, 2010]. This material is well suited to analysis with a microcalorimeter spectrometer.

- U and Pu oxide powders are produced from aqueous solutions. The powders are packed into cans for storage and this material, which is the primary

output of the facility, must be carefully measured. Current NDA measurement uncertainties of this material are 0.8% or slightly better [Johnson, 2009] and rely on neutron and HPGe measurements [Johnson, 2010]. This purified and homogeneous material is extremely well matched to more precise microcalorimeter analysis.

- MOX fuel is fabricated. Oxide powders are blended to achieve the target Pu/U ratio and then pelletized. Pellets are loaded into fuel rods and fuel rods are grouped into assemblies. Presently, the uncertainty in the Pu content of the fuel assemblies is about 10 %, which is alarmingly large [Johnson, 2009]. Fresh MOX fuel is free of fission products so each step of the MOX fabrication process is well suited to microcalorimeter analysis.

It is worth mentioning a more speculative but potentially high-payoff application. Presently, no NDA technique can determine ^{242} Pu content even though this isotope can comprise 10% of the total Pu in material with a long neutron exposure history [Bates, 2015]. It has recently been shown that microcalorimeters can directly measure a low energy gamma-ray near 45 keV from ^{242}Pu [Bates, 2015]. While an important proof-of-principle, this measurement required 12 days and unusual source material depleted of other Pu isotopes. Additional work on this topic is needed to determine if it could be an effective method for realistic materials. MOX material after the Pu stream is purified of Am is ideal for such measurements.

Reprocessing by pyroprocessing is of interest for the future for several reasons including proliferation resistance and potentially easier waste handling [Lee, 2013]. In brief, pyroprocessing consists of head-end steps, electroreduction, electrorefining, cathode material cleanup, and waste handling. Electroreduction and electrorefining are performed in molten salts. Since large-scale pyroprocessing is novel, research is needed to devise adequate safeguards. In the head-end processing, voloxidation and milling are used to declad the fuel and produce a highly homogenous oxide powder prior to electroreduction. The homogeneity of this powder makes it well suited to gamma-ray and self-fluoresced x-ray measurements [Simpson, 2016], although the presence of fission products is likely to prevent isotopic analysis as discussed above. Electroreduction and electrorefining are conducted at very high temperature and thus are unlikely to be directly observable with gamma-ray spectroscopy. Nonetheless, there are related possibilities. Typically, all the transuranic elements (TRUs) are collected on a shared cathode during electrorefining. This complex solid is well suited to microcalorimeter gamma-ray analysis. If inhomogeneity or residual salt prevent mass determination, it may still be possible to confirm normal refining operation by comparing the spectrum from an individual batch to prior data. A malicious change in refining parameters to isolate Pu will affect the observed spectral ratios. The final oxide or metal product as well as the various waste streams are also well matched to gamma-ray analysis, just as in an aqueous plant. Finally, materials accounting requires measurement of TRUs left in the salt (which is reused) after a materials batch is processed. Extracted salt samples are well matched to high-resolution gamma-ray analysis.

Another important application is the idea that measurements performed with microcalorimeters can likely improve analysis by conventional HPGe. This could include using a detailed microcalorimeter measurement to constrain spectral analysis parameters in lower-resolution HPGe data (for example, relative peak amplitudes). The high resolution of microcalorimeter detectors could be used to improve knowledge of the x-ray line widths, which is a non-negligible contributing factor to total measurement uncertainty for HPGe analysis. Similarly, improved knowledge of gamma-ray energies (perhaps relative to each other, rather than absolute) from microcalorimeter measurements would address another significant factor of uncertainty for HPGe.

In the near term, the obvious location for our first steps into the realm of an operating nuclear facility is the H-canyon complex at Savannah River Site. Many of the application scenarios identified above can be tested there at some level. Potential microcalorimeter measurements at the F/H-canyon analytical laboratory were outlined in a recently approved NEUP research proposal. If we are fully successful in measuring elemental and isotopic ratios with 0.2 % uncertainty, then nuclear safeguards will be transformed since NDA can then be substituted for DA in many scenarios. If obstacles to achieving 0.2 % uncertainty emerge, it still seems very likely that microcalorimeter measurements will surpass the accuracy of NDA presently achievable with HPGe. It also seems virtually certain that we will be able to generate improved x-ray and gamma-ray fundamental parameters and that this information will reduce systematic errors in a wide range of HPGe measurements.

Key points from this section:

- *Microcalorimeter detectors have clear measurement applications at many points of a reprocessing stream.*

- *Our target application space is near real-time analysis by x-ray and gamma-ray spectroscopy providing uncertainty limits approaching those of traditional destructive analysis techniques.*

- *Microcalorimeters can potentially improve conventional HPGe spectral analysis by constraining model parameters and improving knowledge of constants of nature.*

7. Future Direction

The summary discussion above has identified at least three key focus areas for future development: 1) improved sensor arrays containing more and/or faster pixels, 2) reduction of limiting systematic uncertainties, and 3) technology demonstration at a real nuclear facility. On the first point the path forward is relatively well-defined. To be truly competitive with HPGe in terms of detection efficiency and counting times, larger microcalorimeter arrays are absolutely

necessary. The final 256-pixel array was operated near, and sometimes beyond, TDM operational limits. More recent work has quadrupled the TDM sampling frequency and will alleviate prior performance issues observed in the realm of high count rates and high photon energies. Thousand-pixel arrays can be envisioned with currently available technology by simply expanding the number of multiplexed columns. At some level, though, this begins to look impractical using TDM methods, as even the MxN wire count advantage and total bandwidth required to collect and record the pulse data become increasingly large. Here is where the development of microwave multiplexing becomes critical for arrays with thousands of pixels. Microwave multiplexing reduces the total wire count even further, reading all pixels simultaneously with a single line, and removing the need to maintain SQUID flux loop lock. Initial work on this topic has progressed in the form of the University of Colorado SLEDGEHAMMER instrument, and the stand-up of a cryostat at LANL dedicated to microwave multiplexing work. We identify further development of microwave multiplexing as a key step towards larger microcalorimeter arrays.

On the topic of total measurement uncertainty, the path is less clear. While we are used to tackling hard technical challenges, the source of limiting systematic uncertainties occurs in part not from within our own technology or data, but derives from external factors and models that were adopted from elsewhere. Specifically, we identified the problems of model discrepancy and nuclear data as limiting factors. Both of these topics are hard.

Improving model discrepancy for spectral peak fitting will benefit from improved uniformity of pixel performance and energy response, leading to more reproducible peak shapes and smaller calibration offsets. A second necessary model describes the system being measured (source attenuation, detector efficiency, etc.). Whether such a model can ever provide less than 1 % error from the actual measured system is presently unknown. In both cases, the use of simulated data seems like a logical approach to quantify such effects. While high-fidelity Monte Carlo simulation has previously been used with some success, development of a faster, simpler, low-fidelity analytical model to easily generate synthetic spectra may be appropriate.

How to reduce the limits imposed by uncertainties in constants of nature is perhaps the least well-developed aspect of the path forward. Improved measurements of nuclear data would require new, exceptionally well-controlled experiments with specially prepared samples having rigorous pedigree. Treatment of constants of nature as calibration parameters would require a large library of spectra from which to derive the adjusted values, and this is not practical with our current library of about 8 high-statistics spectra. New, larger sensor arrays, coupled with measurement campaigns at nuclear facilities is one way to improve on this situation. Finally, there is the idea of reformulating the analysis problem. Instead of requiring absolute branching fractions, perhaps we can reassess the problem in terms of ratios of branching fractions, taking inspiration from the fact that sometimes a ratio of values can be known much more precisely than the two values themselves. Could the Pu isotope ratios be calculated using ratios of branching fractions having much smaller uncertainties than the individual branching fractions

themselves? This is speculative, and further derivation at a more detailed level is needed.

Lastly, it will be highly valuable to demonstrate the microcalorimeter technology in a real operation nuclear facility. This will present a more realistic operational environment, using samples taken directly from relevant processing streams, and an opportunity to increase the total body of data available to address the total measurement uncertainty problem. The F/H-canyon analytical laboratories at SRS are the logical place to pursue such measurements. Material is available from a variety of points in the reprocessing stream, and HPGe and MS measurements are routinely available for comparison and validation of the microcalorimeter measurements. Such measurements have been outlined as part of a recent NEUP proposal.

Key points from this section:

- *Larger sensor arrays are critical and achievable. Microwave multiplexing has a key enabling role to play.*

- *Reduction of limiting systematic uncertainties is required but challenging.*

- *H-Canyon presents the logical location for initial demonstration measurements in an operating nuclear facility.*

8. Project History

The LANL/NIST effort to develop microcalorimeters for gamma-ray spectroscopy began in 2005 with the acquisition of a Pu spectrum containing a few thousand counts from a single sensor [Ullom, 2005]. The first multi-pixel array (16 pixels) followed in 2006, along with the first demonstration of multiplexing [Ullom, 2007]. Around this time the use of GEANT4 Monte Carlo simulations was developed to guide the technology development and aid with interpretation of the data [Hoover, 2007][Hoover, 2009c]. 2007 saw the release of an important publication demonstrating high-resolution performance from a multiplexed array, reporting an average energy resolution of 47 eV FWHM at 103 keV from measurements at NIST [Doriese, 2007]. Subsequent data acquired at LANL resulted in the best reported energy resolution, 22 eV FWHM at 97 keV, and the first multiplexed Pu spectrum [Bacrania, 2009]. In 2008 we began working with a 66-pixel array having several important developments including the use of multiple posts to attach the absorber and TES to reduce interaction position dependent effects, an increased sensor heat capacity to extend the dynamic range from 100 keV to 200 keV, an improvement in response linearity, and an increase in absorber size for improved stopping power [Jethava, 2009b][Hoover, 2009]. This array was also the first to make use of a "flip-chip bonding" method to attach the absorbers to the TESs, replacing tedious by-hand methods and resulting in improved functional sensor yield. At this time, Pu

spectra with ~10^5 counts were being collected. A measurement demonstrating the microcalorimeter ability to cleanly separate the ^{235}U and ^{226}Ra lines at 186 keV was performed [Hoover, 2009]. Also in 2008, following the acquisition of Pu spectra with more counts, efforts in spectral analysis began, initially attempting to apply existing FRAM HPGe analysis code to microcalorimeter data [Karpius, 2009][Vo, 2008].

2009 saw the first fully populated 256-pixel array [Hoover, 2011]. The array incorporated two types of sensors with dynamic range of either 100 keV or 200 keV. Multiplexing capability at that time was able to support simultaneous readout of 160 pixels. Some issues related to thermal expansion were uncovered and subsequently resolved in later designs. The first work on extracting pulse heights from high count-rate data also occurred around this time [Tan, 2009]. Also in 2009, important exploratory measurements on determining Pu content in head-end irradiated fuel using self-induced x-ray fluorescence were performed, using data from HPGe detectors and simulations to assess the potential of microcalorimeter detectors for this application [Hoover, 2009b]. We also began to realize certain challenges associated with the spectral analysis of multi-pixel data concerning spectral peak shapes and energy calibration [Hoteling, 2009]. We began to study thermal crosstalk effects in detail [Jethava, 2009].

Around 2011, work culminated in the construction of a fully instrumented 256-pixel array, with a uniform sensor design having 200 keV dynamic range, and supporting multiplexing technology capable of simultaneous readout of all pixels. Measurements at NIST recorded 92% of pixels functional with average resolution of 53 eV FWHM at 103 keV. These results lead to an important technical review paper [Bennett, 2012]. After moving the 256-pixel array to LANL, similar results were observed and it became possible to collect Pu spectra having more than ~10^7 total counts [Winkler, 2015].

These data, along with those collected from prior generations of sensor arrays (over 1300 hours of integrated measurement time), allowed us to begin a serious look at measurement uncertainty. This led to a complete rewrite of spectral analysis codes and a detailed comparison of statistical uncertainty for HPGe and microcalorimeter measurements in 2012 [Hoover, 2013]. Also at this time new algorithms for pulse-processing in high event-rate scenarios were developed, showing that pile-up pulses could be used for analysis [Alpert, 2013]. In 2014, as a follow-on to the paper on statistical uncertainty, we reported on systematic uncertainty and identified limiting factors of the analysis for HPGe and microcalorimeter data [Hoover, 2014]. We also demonstrated operation of the 256-pixel array for total event rates exceeding 1 kcps, and published a summary of Pu measurements using the 256-pixel array [Winkler, 2015]. The use of microwave multiplexing was demonstrated, a promising new technology for the readout of future sensor arrays having thousands of pixels [Noroozian, 2013][Bennett, 2014].

This brief history summarizes a rapid progression from the single-pixel proof-of-concept measurement in 2005, to a fully-multiplexed 256-pixel array capable of 1 kcps event rate in 2014. The advances in sensor array technology allowed for the acquisition of Pu spectra with ever-increasing total counts in shorter periods of time. The collection of high-statistics spectra from Pu isotopic standards led to development of spectral analysis methods and a quantitative assessment of

total measurement uncertainty. Multiplexing technology was also advanced at a rapid pace. The size of sensor arrays that is now possible led to investigations of microwave multiplexing as an improvement over conventional multiplexing to enable arrays with many thousands of pixels, continuing to drive detection efficiency up and measurement times down.

Key points from this section:

- *In 2005 we operated a single pixel detector. By 2011 we were operating a fully multiplexed 256-pixel array*

- *In 2005 we had a Pu spectrum with a few thousand counts. By 2013, we had collected Pu spectra exceeding 1300 hours integrated measurement time with tens of millions of counts from a number of calibrated Pu standards.*

- *In 2005, we had a total event rate of a few cps from a single pixel. By 2014, we demonstrated 256-pixel array operation at over 1 kcps.*

- *Spectral analysis code was developed from scratch and used to quantify statistical and systematic uncertainties.*

9. References

Alpert BK, et al., "Note: operation of gamma-ray microcalorimeters at elevated count rates using filters with constraints." *Rev. Sci. Instrum*., 84 (2013) 056107

Bacrania MK, et al., "Large-area microcalorimeter detectors for ultrahigh resolution x-ray and gamma-ray spectroscopy," *IEEE Trans. Nucl. Sci.,* (2009) 2299–2302

Bates C, "Development of metallic magnetic calorimeters for nuclear safeguards applications." Ph.D. Thesis, Berkeley (2015)

Bennett DA, et al., "A high resolution gamma-ray spectrometer based on superconducting microcalorimeters." *Rev. Sci. Instrum*., 83 (2012) 093113

Bennett DA, et al., "Integration of tes microcalorimeters with microwave squid multiplexed readout." *IEEE Trans. Appl. Supercond*., 25 (2014) 2101405

Burr T, Sampson T and Vo D, "Statistical evaluation of FRAM gamma-ray isotopic analysis data." *Appl. Rad. Isot.,* 62 (2005) 931–940

Cantor R and Naito H, "Practical x-ray spectrometry with second-generation microcalorimeter detectors." *Microsc. Today*, 20 (2012) 38–42

Croce MP, et al., "Development of Holmium-163 electron capture spectroscopy with transition-edge sensor microcalorimeters." *J. of Low Temp. Phys.,* 184 (2016) 958-968

Deslattes R, et al., "X-ray transition energies: New approach to a comprehensive evaluation," *Rev. Mod. Phys.,* 75 (2003) 35–99

Doriese WB, et al., "A 14-pixel, multiplexed array of gamma-ray micro-calorimeters with 47 eV energy resolution at 103 keV." *Appl. Phys. Lett.,* 90 (2007) 191910

Durst PC, et al., "Advanced safeguards approaches for new reprocessing facilities." PNNL-16674 (2007)

Hoover AS, et al., "Simulating the response of ultra-high energy resolution X- and Gamma-ray

microcalorimeter detectors." *Nuclear Science Symposium Conference Record 2007 IEEE* (2007) 847-849

Hoover AS, et al., "Microcalorimeter arrays for ultra-high energy resolution X- and gamma-ray detection." *J. of Radioanal. and Nucl. Chem.,* 282 (2009) 227-232

Hoover AS, et al., "Measurement of plutonium in spent nuclear fuel by self-induced X-ray fluorescence." *Proceedings of the INMM 50th Annual Meeting* (2009b)

Hoover AS, et al., "Application of GEANT4 to the Simulation of High Energy-Resolution Microcalorimeter Detectors." *IEEE Transactions on Nuclear Science*, vol. 56 (2009c) 2294-2298

Hoover AS, et al., "Large microcalorimeter arrays for high-resolution X- and gamma-ray spectroscopy." *Nucl. Instrum. and Meth. in Phys. Res. A,* 652 (2011) 302-306

Hoover AS, et al., "Determination of plutonium isotopic content by microcalorimeter gamma-ray spectroscopy." *IEEE Trans. on Nucl. Sci.,* 60 (2013) 681-688

Hoover AS, et al., "Uncertainty of plutonium isotopic measurements with microcalorimeter and high-purity germanium detectors." *IEEE Trans. on Nucl. Sci.,* 61 (2014) 2365-2372

Hoover AS, et al., "Measurement of the $^{240}Pu/^{239}Pu$ mass ratio using a transition-edge-sensor microcalorimeter for total decay energy spectroscopy." *Anal. Chem.,* 87 (2015) 3996-4000

Horansky RD, et al., "Superconducting absorbers for use in ultra-high resolution gamma-ray spectrometers based on low temperature microcalorimeter arrays." *Nucl. Instrum. and Meth. in Phys. Res. A,* 579 (2007) 169-172

Horansky RD, et al., "Identification and elimination of anomalous thermal decay in gamma-ray microcalorimeters." *Appl. Phys. Lett.,* 103 (2013) 212602

Hoteling N., et al., "Issues in energy calibration, nonlinearity, and signal processing for gamma-ray microcalorimeter detectors." *AIP Conf. Proc*., 1185 (2009) 711-714

Hubbell J, "Photon mass attenuation and energy-absorption coefficients from 1 keV to 20 MeV," *Int. J. Appl. Radiat. Isot.*, 33 (1982) 1269–1290

Irimatsugawa T, et al., "High energy gamma-ray spectroscopy using tes with a bulk tantalum absorber." *IEEE Trans. Appl. Supercond*., 25 (2014) 2101303

Jethava N, et al., "Characterization of thermal cross-talk in a gamma-ray microcalorimeter array." *AIP Conf. Proc.,* 1185 (2009) 34-37

Jethava N, et al., "Improved isotopic analysis with a large array of microcalorimeters." *IEEE Trans. of Appl. Supercond.,* 19 (2009b) 536-539

Johnson S, "The safeguards at reprocessing plants under a fissile material (cutoff) treaty." Research Report 6, International Panel on Fissile Materials (2009)

Johnson SJ and Ehinger M, "Designing and operating for safeguards: lessons learned from the Rokkasho reprocessing plant (RRP)." PNNL-19626 (2010)

Karpius PJ, et al., "A first application of the FRAM isotopic analysis code to high-resolution microcalorimetry gamma-ray spectra." *IEEE Trans. on Nucl. Sci.,* 56 (2009) 2284-2289

Krause MO and Oliver JH, "Natural widths of atomic K and L levels, Kα X-ray lines, and several kll auger lines." *J. Phys. Chem. Ref. Data,* vol. 8, no. 2 (1979) 329–338

Lee DW, "Spectral analysis of cryogenic microcalorimeter data with modified peak shapes." *Proceedings of the INMM 52nd Annual Meeting* (2011)

Lee H et al., "Current status of pyroprocessing development at KAERI." *Science and Technology of Nuclear Installations* (2013) 343492

Moseley SH, Mather JC and McCammon D, "Thermal detectors as x-ray spectrometers." *J. Appl. Phys.,* 56 (1984) 1257–62

Noroozian O, et al., "High-resolution gamma-ray spectroscopy with a microwave-multiplexed transition-edge sensor array." *Appl. Phys. Lett*., 103 (2013) 202602

O'neal HR and Phillips NE, "Low-temperature heat capacities of indium and tin." *Phys. Rev*., 137 (1965) A748

Rabin MW, “National and international security applications of cryogenic detectors – mostly nuclear safeguards.” *AIP Conf. Proc.*, 1185 (2009) 725-732

Rettschlag M, Berndt R and Mortreau P, “Measurement of photon mass attenuation coefficients of plutonium from 60 to 2615 keV.” *Nucl. Instrum. Meth. Phys. Res. A,* 581 (2007) 765–771

Salem S, Panossian S and Krause R, “Experimental K and L relative X-ray emission rates,” *Atomic Data and Nuclear Tables,* 14 (1974) 91–109

Sampson T and Gunnink R, “The propagation of errors in the measurement of plutonium isotopic composition by gamma-ray spectroscopy.” Los Alamos Nat. Laboratory Report LA-UR-83-1520 (1983)

Sampson TE, Nelson GW, and Kelley TA, “FRAM: A versatile code for analyzing the isotopic composition of plutonium from gamma-ray pulse height spectra.” Los Alamos Nat. Laboratory Rep. LA-II720-MS (1989)

Sampson TE, Kelley TA and Vo DT, “Application guide to gamma-ray isotopic analysis using the FRAM software.” Los Alamos Nat. Laboratory report LA-14018 (2003)

Scheinman A, "Calling for Action The Next Generation Safeguards Initiative," *Nonproliferation Review* 16 (2009) 257-267

Sellers GJ, Anderson AC and Birnbaum HK, “Anomalous heat capacities of niobium and tantalum below 1 k.” *Phys. Rev. B,* 10 (1974) 2771

Szymkowiak A., et al., “Signal processing for microcalorimeters.” *J. Low Temp. Phys*., 93 (1993) 281

Tan H, et al., "High rate pulse processing algorithms for microcalorimeters." *AIP Conf. Proc.,* 1185 (2009) 294-297

Thompson P, Cox DE, and Hastings JB, “Rietveld refinement of debye-scherrer synchroton X-ray data from Al_2O_3.” *J. Appl. Cryst.,* 20 (1987) 79–83

Trubey D, Berger M and Hubbell J, “Photon cross sections for ENDF/B-VI.” Oak Ridge National Laboratory report CONF-890408-4, OSTI ID 6452481 Oak Ridge Nat. Lab., Oak Ridge, TN, USA, Tech. Rep. (1989)

Qaim SM, Editor, “Evaluated Nuclear Structure Data File (ENSDF).” Nuclear Data for Science and Technology, Springer-Verlag, Berlin, Germany (1992)

Ullom JN, et al., "Development of large arrays of microcalorimeters for precision gamma-ray spectroscopy." *Nuclear Science Symposium Conference Record 2005 IEEE,* 2 (2005) 1154-1158

Ullom JN, et al., "Multiplexed microcalorimeter arrays for precision measurements from microwave to gamma-ray wavelengths." *Nucl. Instrum. and Meth. in Phys. Res. A,* 579 (2007) 161-164

Ullom JN, Bennett DA, “Review of superconducting transition-edge sensors for x-ray and gamma-ray spectroscopy.” *Supercond. Sci. Technol.,* 28 (2015) 084003

Vo DT, et al., “Plutonium isotopic analysis of microcalorimeter gamma-ray spectra.” *Trans. of the American Nucl. Soc.,* 98 (2008) 403

Winkler R, et al., “256-pixel microcalorimeter array for high-resolution gamma-ray spectroscopy of mixed-actinide materials.” *Nucl. Instrum. and Meth. in Phys. Res. A*, 770 (2015) 203-210

Zhao K, et al., “International target values 2010 for measurement uncertainties in safeguarding nuclear materials.” ESARDA Bulletin No. 48 (2012)